X-ray Observations of Saturn & Jupiter
Past, Present, and Possible Futures

I. Saturn --- faint enough that simple ideas seem to give a coherent picture

II. Jupiter --- bright enough that simple ideas do not suffice, but faint enough to keep questions open

III. Future hopes --- imaging x-ray spectrometer on S/C in Jovian system

X-ray Emission from the Saturn System

A. Bhardwaj, R. F. Elsner, J. H. Waite, G. R. Gladstone,
T. E. Cravens, G. Branduardi-Raymont, P. G. Ford

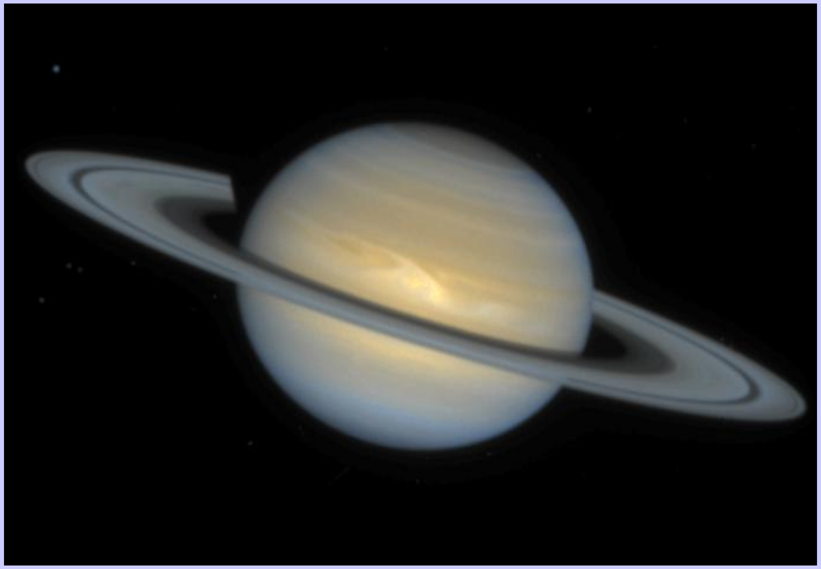

CXO & XMM-Newton X-ray Communities:
J.-U. Ness, J.H.M.M. Schmitt, &
J. Robrade U. Hamburg
G. Branduardi-Raymont, G. Ramsay, MSSL
R. Soria, MSSL-CfA, S. Volk CfA
P. Rodriguez, XMM-Newton SOC
K. Dennerl, V. Burwitz MPE
K. Mori, D. Burrows, G. Garmire Penn State
H. Tsunemi, H. Katayama Osaka U.
A. Metzger, JPL

X-ray Observational History for the Saturn System

EINSTEIN IPC: Gilman et al.			**Ap. J (1986)**
	3 hours on Dec 17, 1979	0.2-3.0 keV	no detection
ROSAT PSPC: Ness & Schmitt			**A&A (2000)**
	1.48 hour on Apr 30, 1992	0.1-1.6 keV	marginal detection
XMM-Newton EPIC-pn: Ness, Schmitt & Robrade			**A&A (2004)**
	6.67 hour on Oct 1, 2002	0.2-2.0 keV	detection & spectra
Chandra ACIS/grating: Mori et al.			**Ap. J. (2004)**
	9.7 hours on Jan 5, 2003		Titan occults Crab;
Chandra ACIS-S: Ness et al.			**A&A (2004)**
	18.2 hours on Apr 14-15, 2003	0.2-2.0 keV	spectrum & spatial
Chandra ACIS-S: Bhardwaj et al.			**Ap. J. Lett. (2005a,b)**
	10.4 hours on Jan 20, 2004	0.24-2.0 keV	spectrum, spatial,
	10.1 hours on Jan 26-27, 2004	0.24-2.0 keV	flare, rings
XMM-Newton: Branduardi-Raymont et al.			
	~20 h on Apr 21-22 & on Oct 28-29, 2005	0.2-2.0 keV	

Titan's Occultation of the Crab Nebula

Mori et al. 2004, Ap. J., 607, 1065 measured extent of atmosphere from x-ray absorption consistent with or slightly larger than Voyager observations.

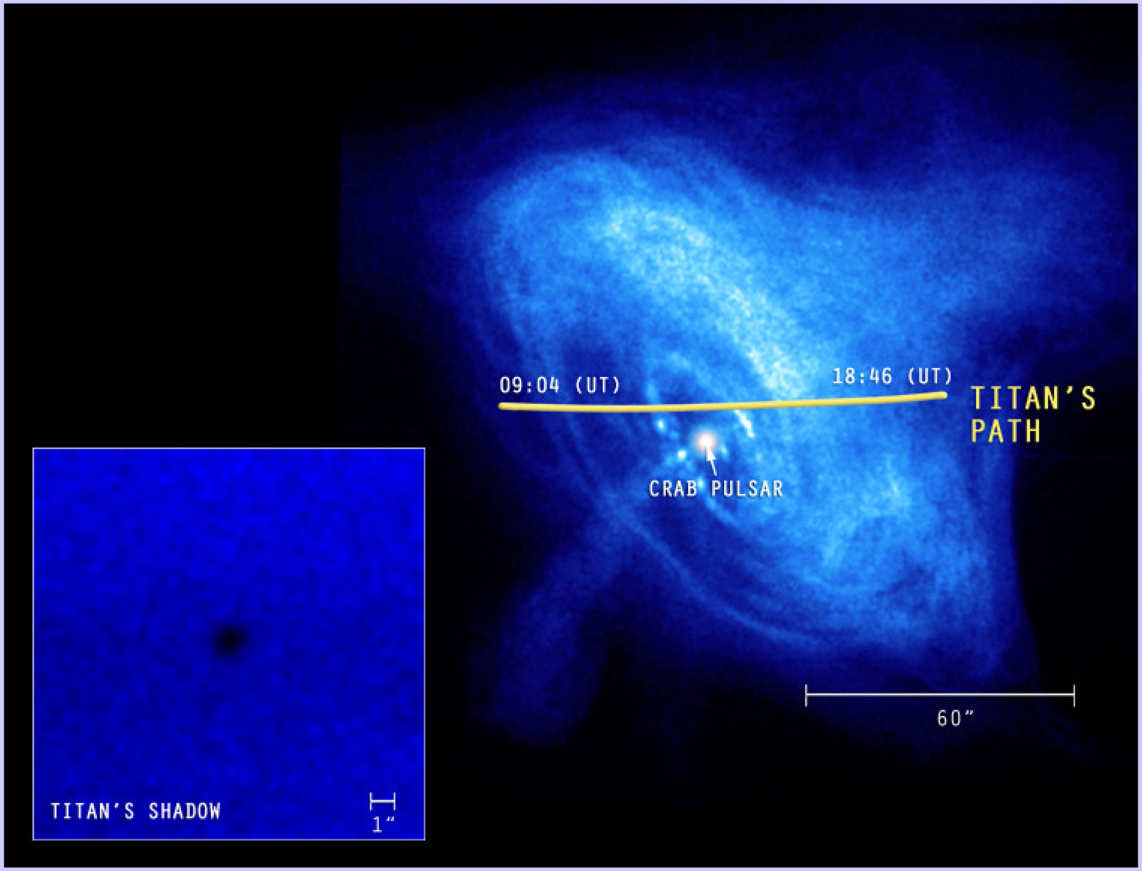

April 14-15, 2003 Chandra ACIS-S Observation of Saturn

Ness et al. 2004, A&A, 418, 337 reported first unambiguous spatially and spectrally resolved x-ray observations of Saturn using Chandra ACIS-S. Spectrum consistent with solar.

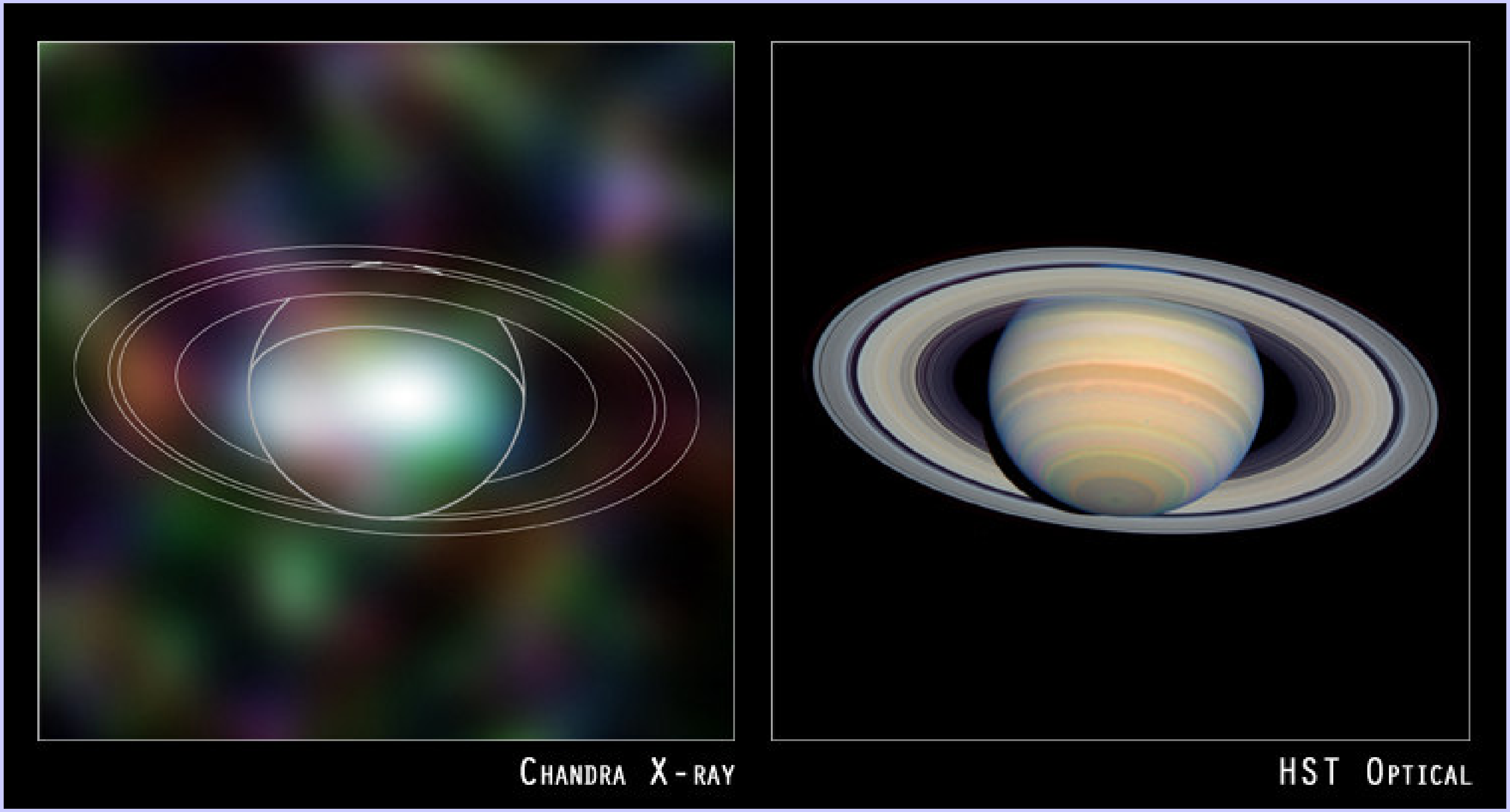

Jan 20 & 26, 2004 Chandra ACIS-S Observations of Saturn

The two observations, only a week apart, look very different.

The 0.24-2.0 counts from the disk excluding the rings and south polar cap are 134 & 32 with 38.4 & 5.2 expected from background. The counts from the south polar cap region are 17 & 6 with 5.2 & 0.4 expected from background. The polar cap spectrum is consistent with the disk but not with Jupiter's auroral spectrum.

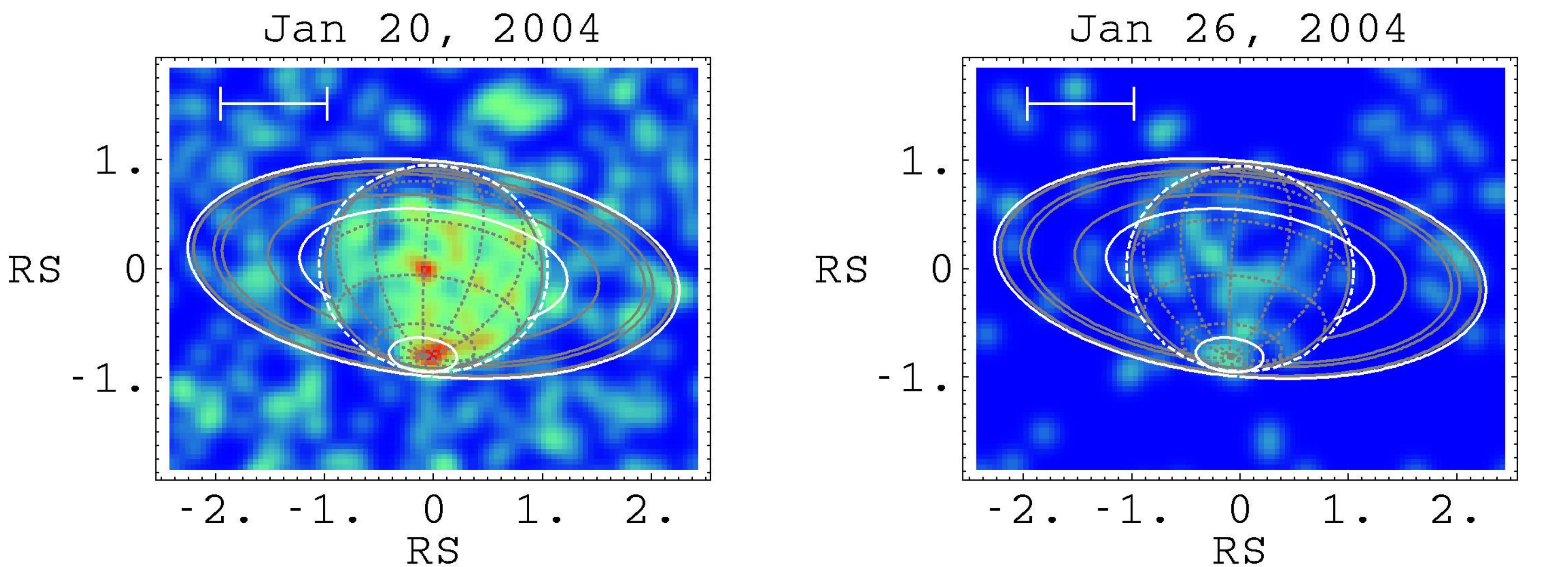

Scale bar is 10"

1 R = $(10^6/4\pi)$ photon / cm^2-s-sr

April 14-15, 2003 Chandra ACIS-S Observation of Saturn

The earlier observation, plotted on same color scale, looks different from the other two.

Scale bar is 10"

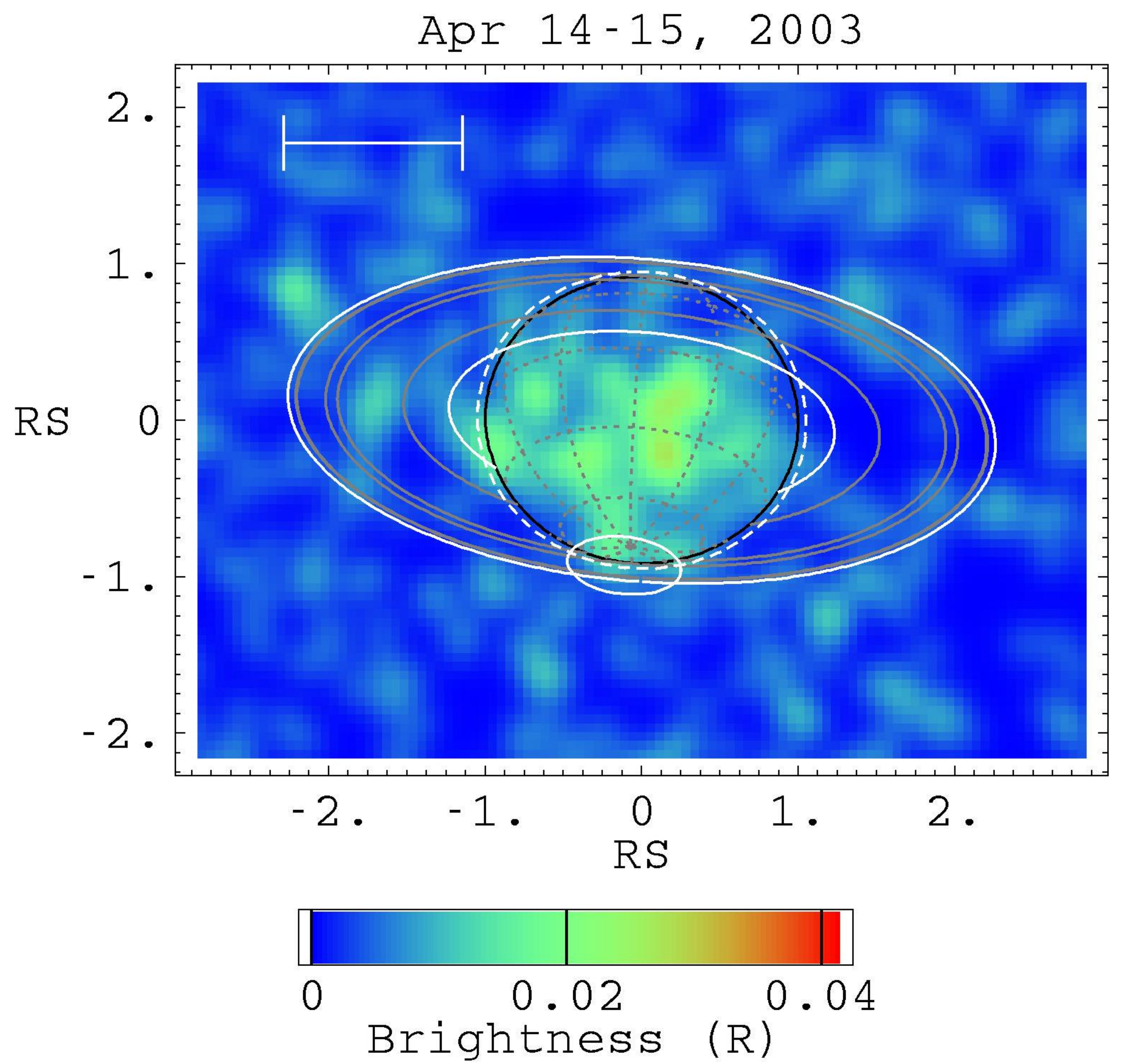

Saturn & Solar X-ray Time Histories on Jan 20, 2004

The background subtracted light curve on Jan 20, 2004, is not constant, and shows a flaring episode near the end of the exposure. When light travel time effects are included, this flare is coincident with an M6.1 solar flare from sunspot 10540 which lasted for ~36 min.

MEKAL Spectral Fits to Jan 20, 2004 & Apr 14-15, 2003 Data

The optically thin, thermal-equilibrium MEKAL model provides a good fit to the Jan 20, 2004, disk spectrum, but requires the addition of an O K line at 0.53 keV for the Apr 14-15, 2004, disk spectrum.

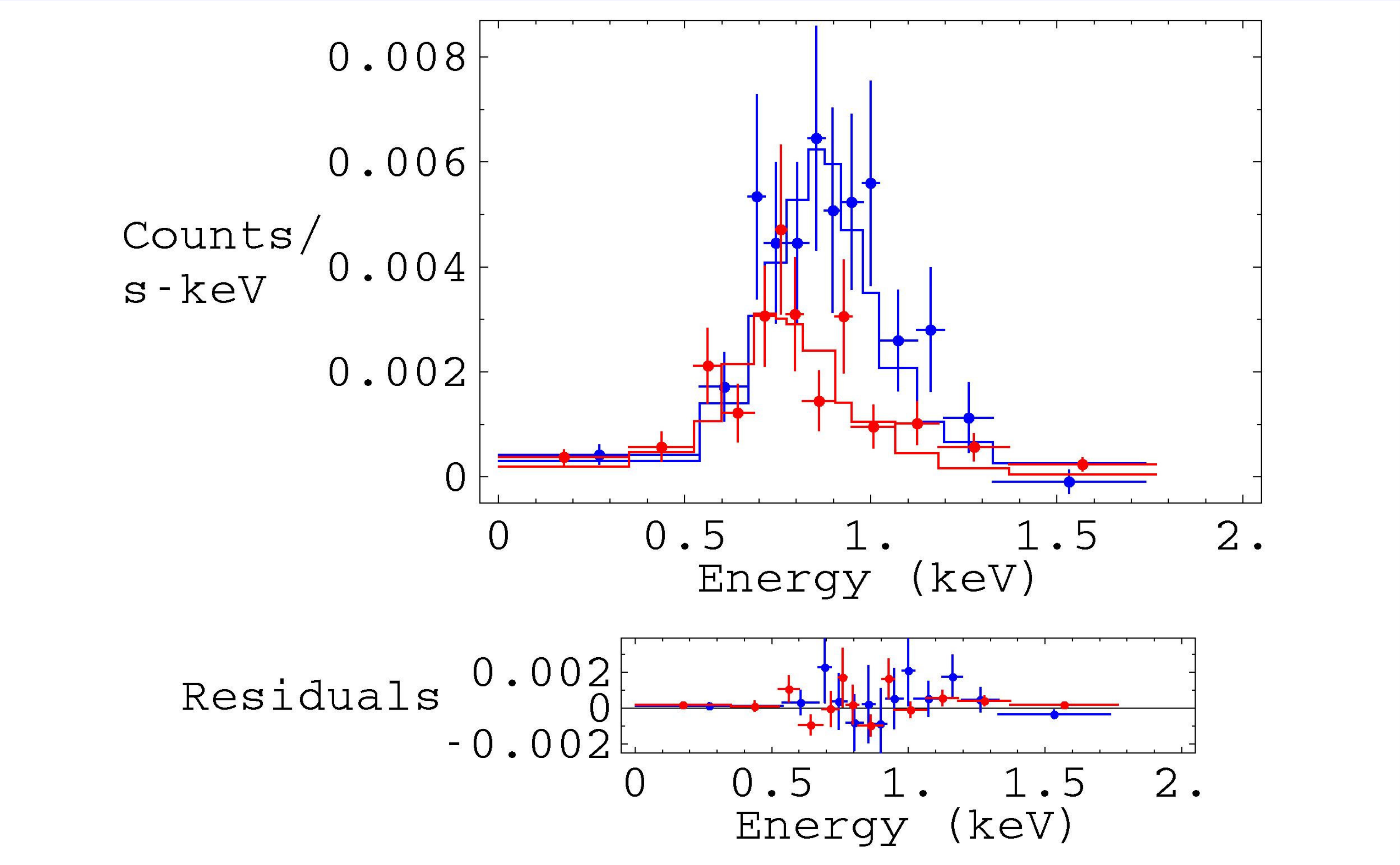

Correlation between X-ray Flux from Saturn & Solar Activity

The 10.7 cm solar flux is used as a proxy for solar activity. The reported x-ray power from Saturn correlates very well with the 10.7 cm solar flux. The evidence points to x-rays from Saturn's disk resulting from scattering of and fluorescence due to solar x-ray emission incident on the disk.

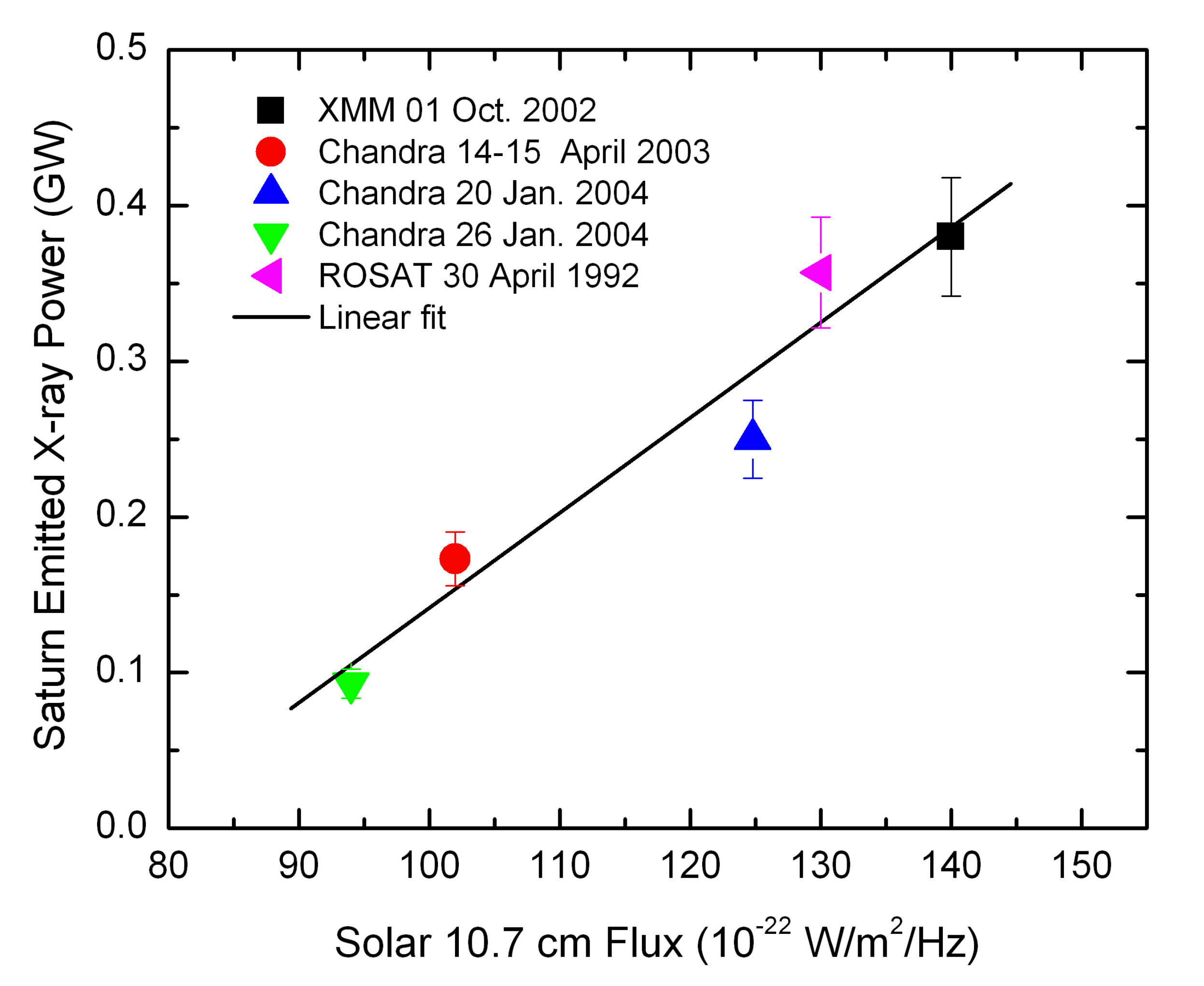

Images of Saturn & Rings in the Energy Band 0.49-0.62

Ness et al. 2004 found a small but significant photon excess on side of the rings in the Apr 14-15, 2003, data.. The image for Jan 20, 2004, confined to the energy band 0.49-0.62 keV definitely shows emission from the rings with an apparent excess from the same side of the rings.

Spatial scale bar is 10"

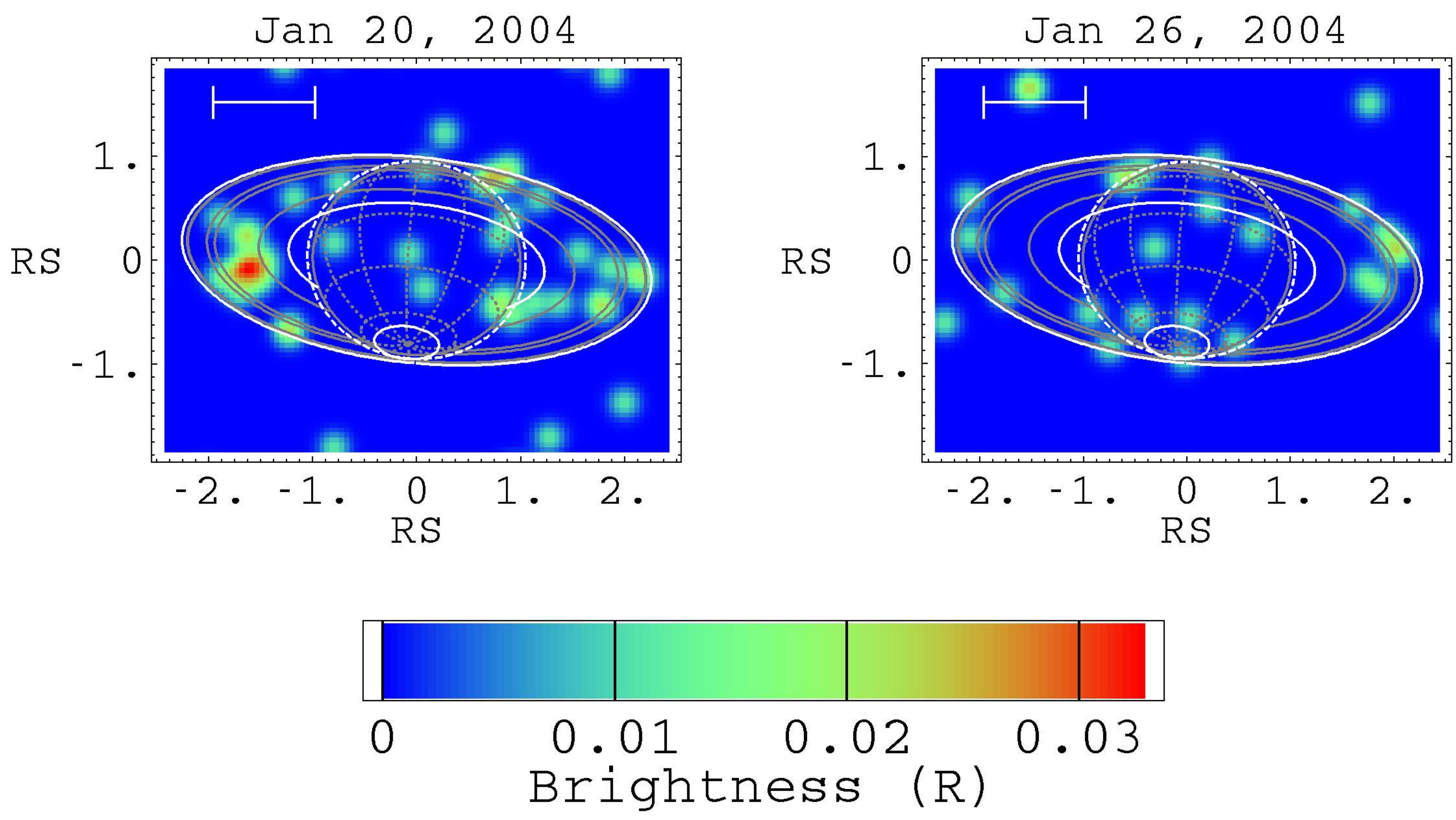

Images of Saturn & Rings in the Energy Band 0.49-0.62 keV

Here is the Apr 14-15, 2003, image in the 0.49-0.62 keV energy band. These images strongly suggest O K fluorescent line emission, consistent with the largely water ice composition of the rings.

Spatial scale bar is 10"

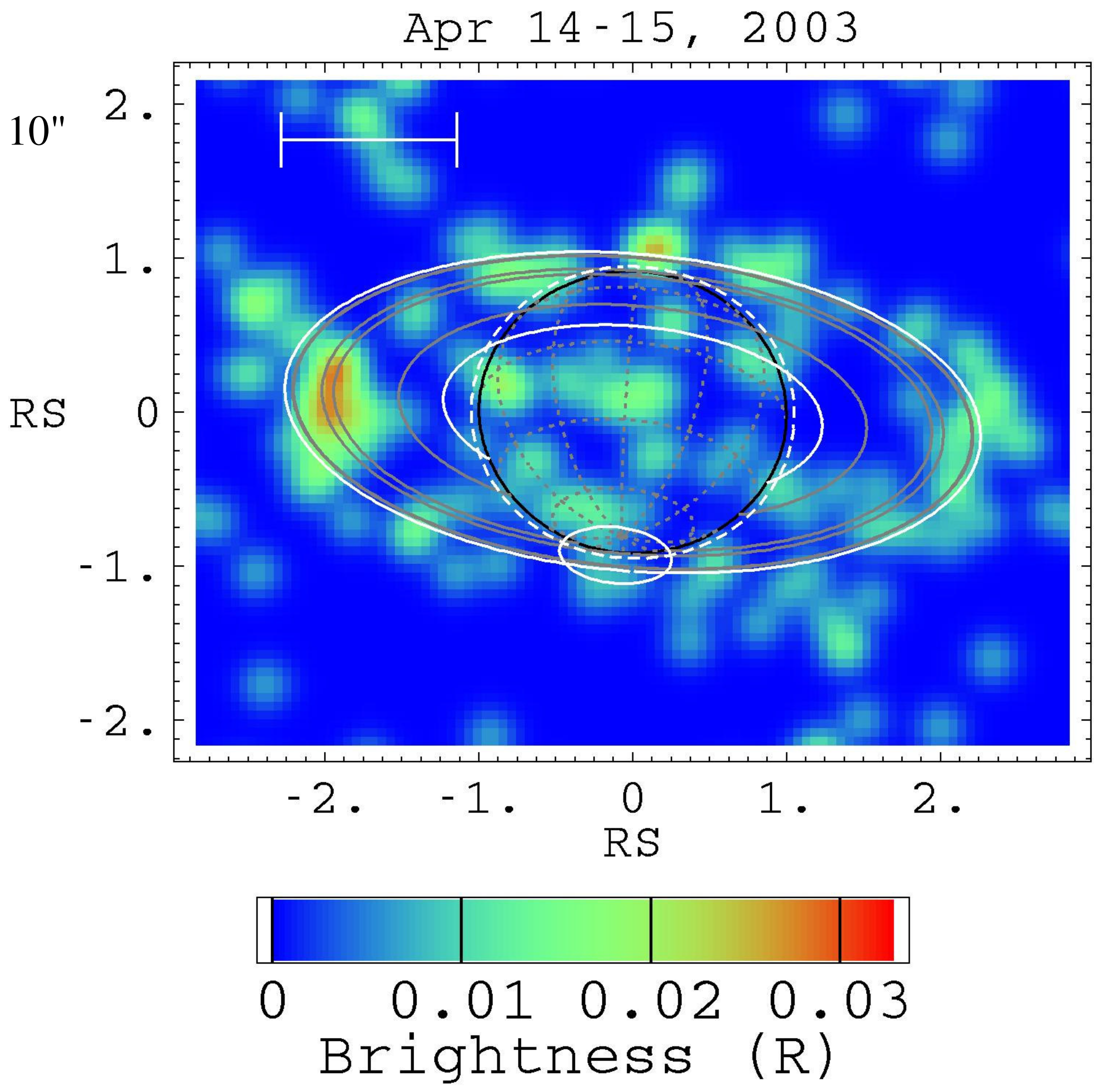

Line Fits to Jan 20, 2004 & Apr 14-15, 2003 Data Confined to Rings

In fact, background subtracted spectra show no evidence for x-ray emission from the rings except in a line with center consistent with neutral O K fluorescence.

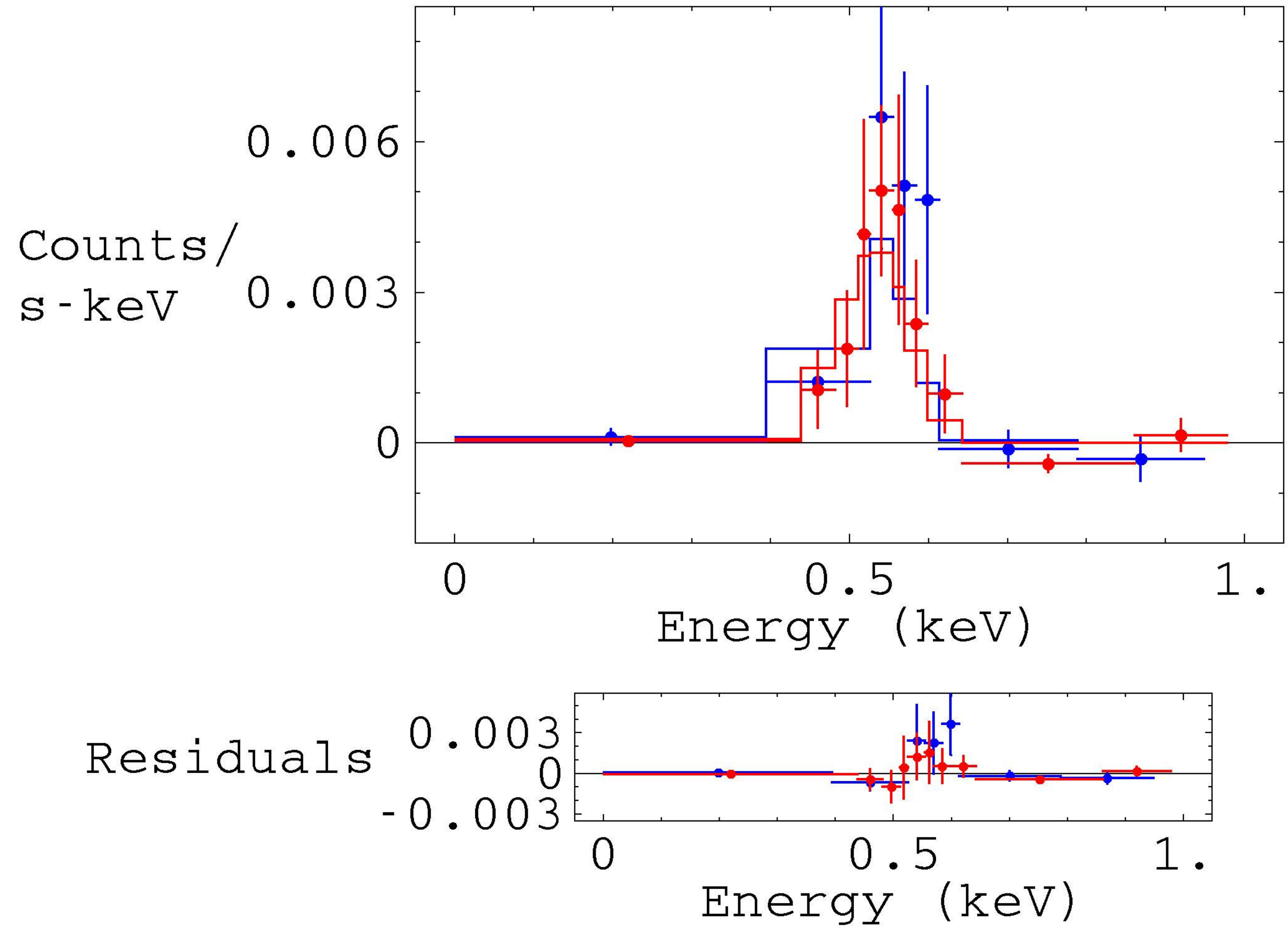

Asymmetry in Ring X-ray Emission ?

Combining the April 14-15, 2003, and Jan 20 & 26, 2004, exposures, the angular distribution of 0.49-0.62 events from the rings, taking into account the exposed projected area and excluding Saturn's planetary disk, provides suggestive but not overwhelming evidence for an East-West asymmetry. There are 13 events in sector 1 (West) and 22 in sector 7 (East). The probability of 22 expecting 13 is 0.002. The dotted curve on the right is proportional to the exposed projected area.

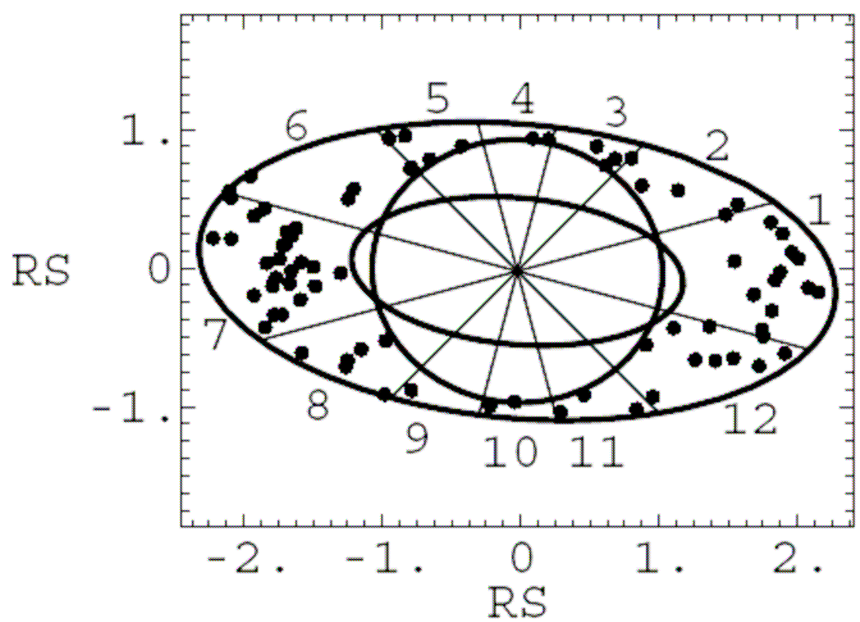

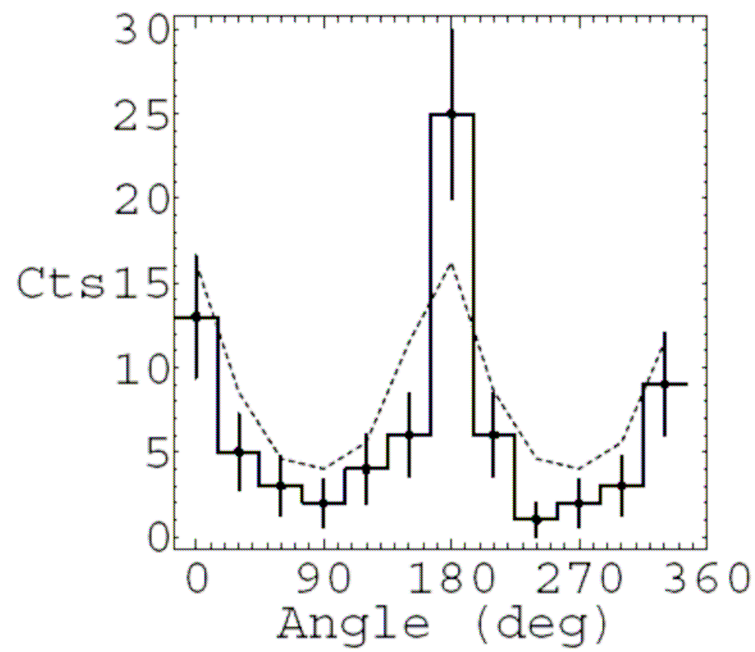

Summary

- X-rays from Saturn flared coincident with the arrival of solar x-rays from an M-class solar flare.

- X-ray spectra consistent with optically thin, thermal-equilibrium emission (but albedo effects not included --- see Cravens et al. 2005, J. Geophys. Res., submitted).

- Variability in Saturn's x-ray emission correlates well with the F10.7 cm flux proxy for solar activity.

- We find no evidence, at the present level of sensitity, for a south polar x-ray auroral.

- We conclude that the x-ray emission from Saturn's planetary disk is the result reprocessing of the incident solar flux in Saturn's atmosphere. This is also largely the case for Jupiter's low-mid-latitude x-ray emission, although the situation is complicated by Jupiter's very non-dipolar magnetic field and its dynamic and active magnetosphere.

- Saturn's rings shine in x-rays in the O K fluorescent line at ~0.53 keV.

- Fluorescent emission due to incident solar x-rays from O atoms in the H_2O icy ring material is the likely source for the ring x-ray emission.

- There possibly is an East-West asymmetry in the ring x-ray emission. If so, its origin is mysterious, as there should be no such asymmetry in the incident solar flux.

X-ray Probes of Jupiter's auroral zones, Galilean moons, and the Io plasma torus

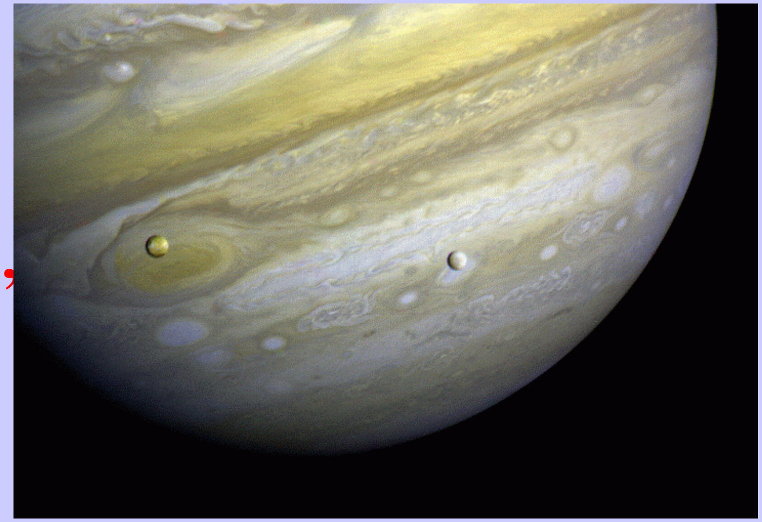

R. Elsner, A. Bhardwaj MSFC; G. R. Gladstone SwRI;
J. H. Waite U. Michigan; T. Cravens U. Kansas; P. Ford MIT;
G. Branduardi-Raymont, Gavin Ramsay MSSL;
B. D. Ramsey MSFC

CXO X-ray Community:
A. Tennant & M. Weisskopf, MSFC
E. Feigelson & G. Garmire, Penn State Univ.
K. Hurley, Univ. of California, Berkeley

XMM-Newton X-ray Community:
R. Soria, MSSL-CfA
P. Rodriguez, XMM-Newton SOC

Planetary Community:
J. F. Cooper, GSFC
R. E. Johnson, Univ. Va.
F. Crary, SwRI
D. Grodent, Univ. of Liege
R. Howell, Univ. of Wyoming
A. Metzger, JPL
T. Majeed, Univ. of Michigan

Feb, 2003, Chandra ACIS-S Image of Jupiter

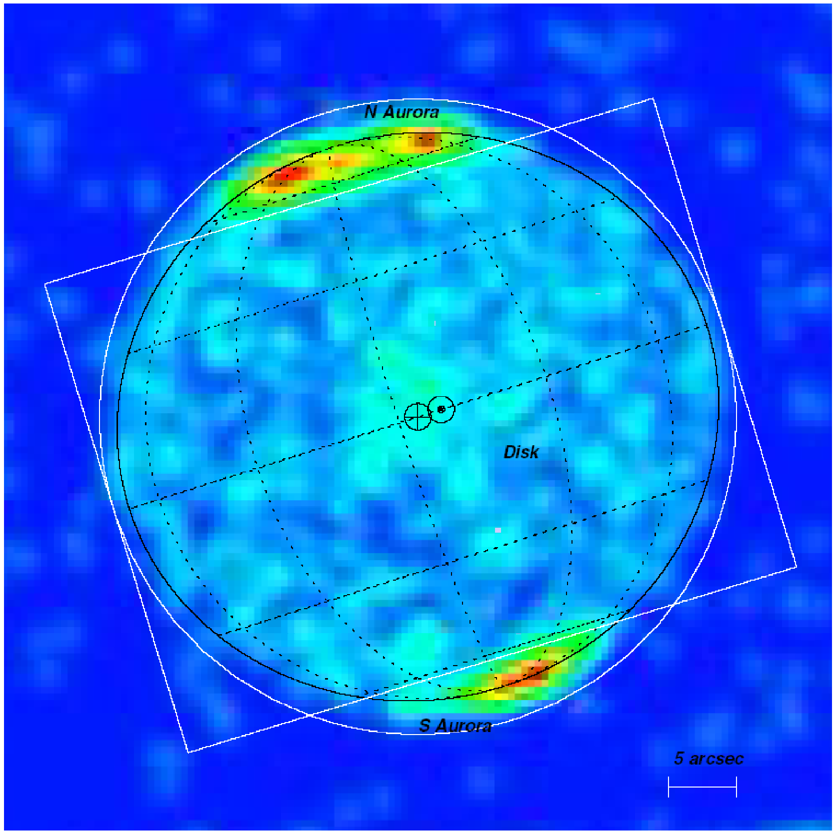

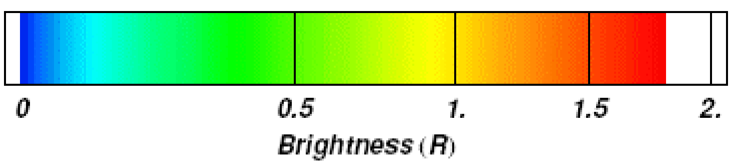

Color coded histogram of ACIS-S (0.25–2.0 keV) events from 24-26 February 2003, observations as seen in a frame moving across the sky with Jupiter, smoothed with a two-dimensional gaussian with $\sigma = 0.738$ arcsec (1.5 ACIS pixel width). The white scale bar in the lower right represents 5 arcsec, and the small circles near the center represent the sub-Earth and sub-solar points. The superimposed graticle shows latitude and longitude lines at intervals of 30°. The total 0.25–2.0 keV count rate inside the dashed circle is 0.034 counts per second, while that within 0.75 Jovian radii but scaled to the size of the planet is 0.024 counts per second. The equivalent background rate derived from events more than 1.2 Jovian radii from the planet's center and scaled to the size of the planet is 0.00088 counts per second, showing the effectiveness of Very Faint mode for suppressing background. The color bar for the figure is in Rayleighs (R).

The planet's emission is about 1/2-2/3 that in Dec, 2000.

X-ray Map in System III Longitude and Latitude

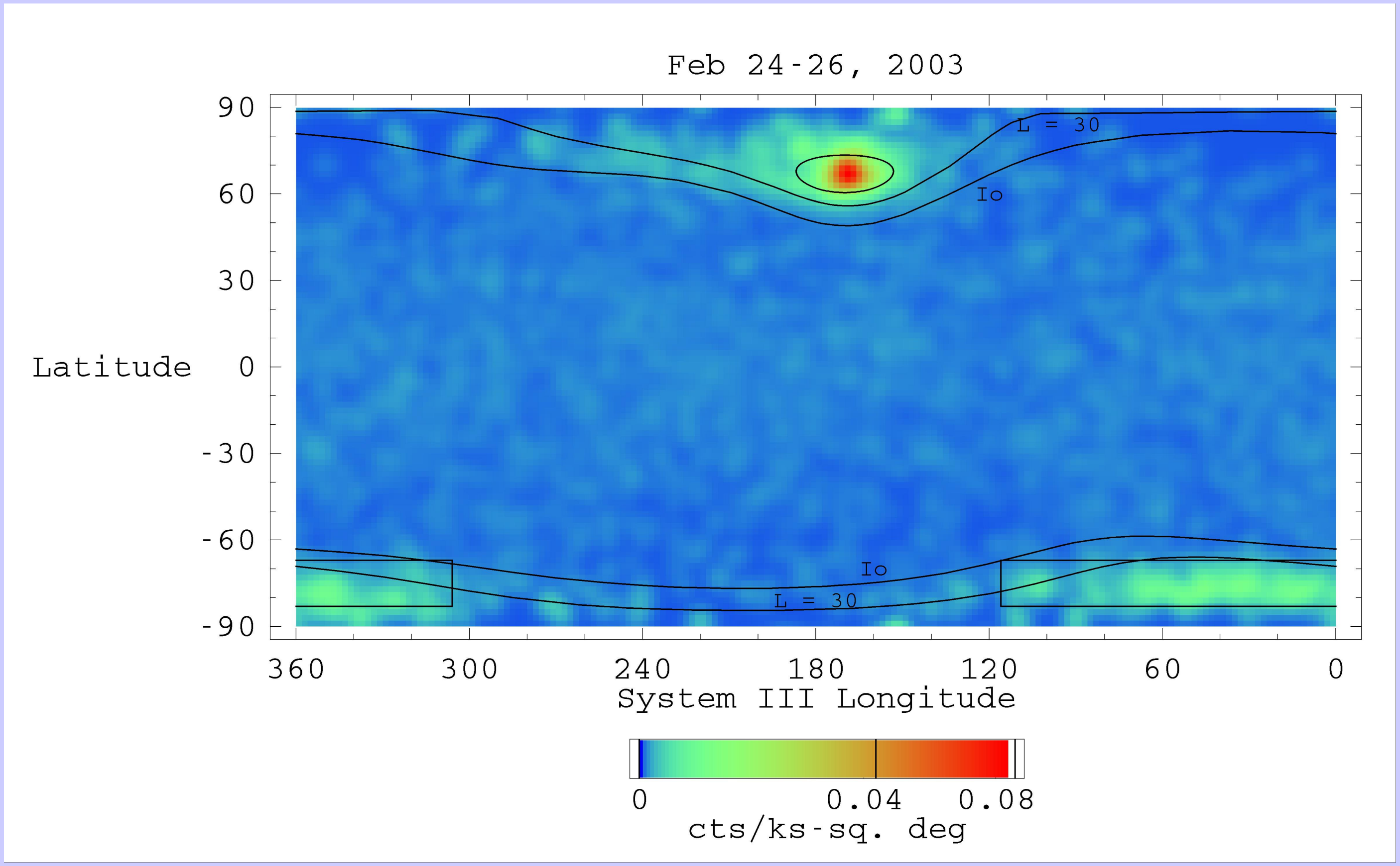

Rate map for the Feb. 24-26, 2003 data, 250-2,000 eV, summed over both ACIS-S exposures and the HRC-I exposure, in System III coordinates, convolved with a two-dimensional gaussian with $\sigma = 1.5°$. The lines crossing the plot from 360° to 0° trace the feet of the Io flux tube and the L = 30 flux tube, as defined by the VIP4 model, in the north and south hemispheres. The color bar of the figure is in counts per kilosecond per square degree.

Distribution of events looking down on the N & S poles

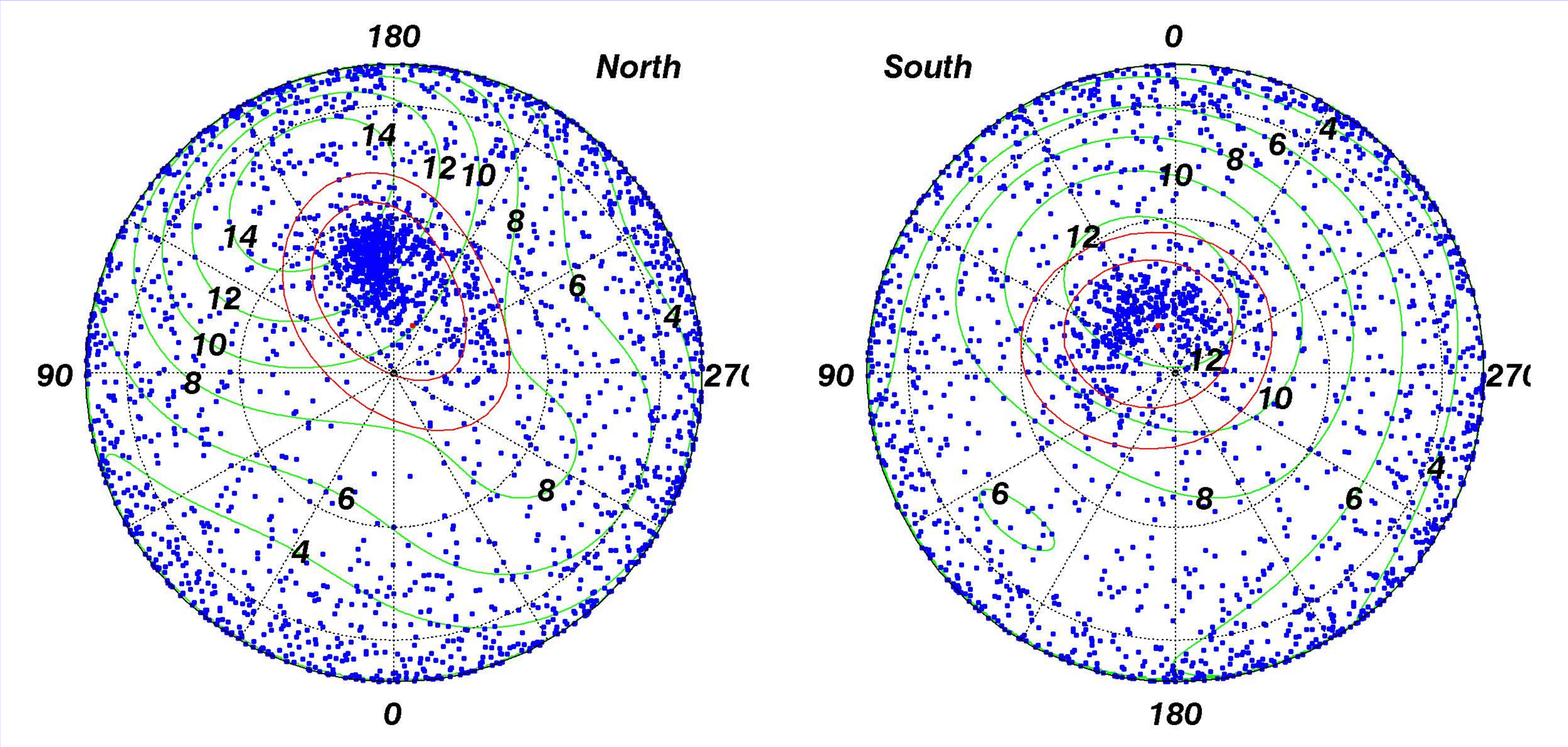

The blue dots represent x-ray events; the red lines the Io and L=30 flux tubes; and the green lines contours of constant surface magnetic field strength. The auroral hot spot in the north and the more spread out auroral emission in the south are apparent. The apparent concentration of events near the equator is a projection effect.

Feb, 2003, Chandra ACIS-S Auroral Spectra

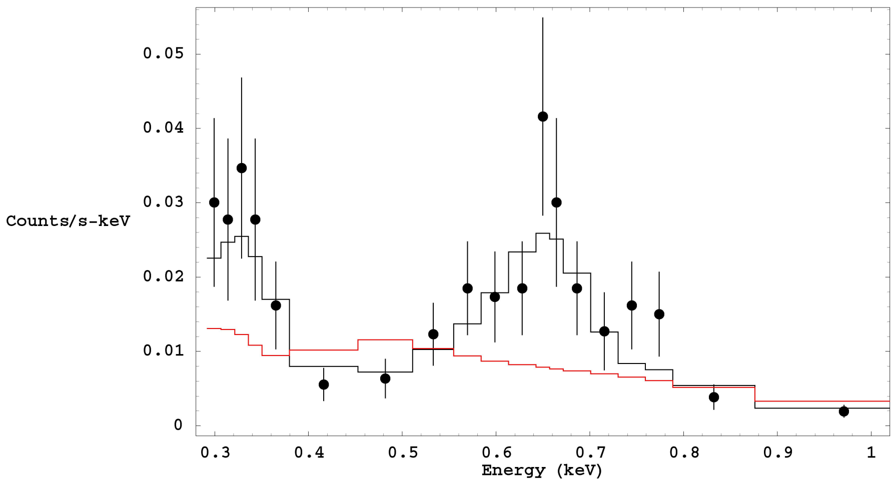

Oxygen & Sulfur

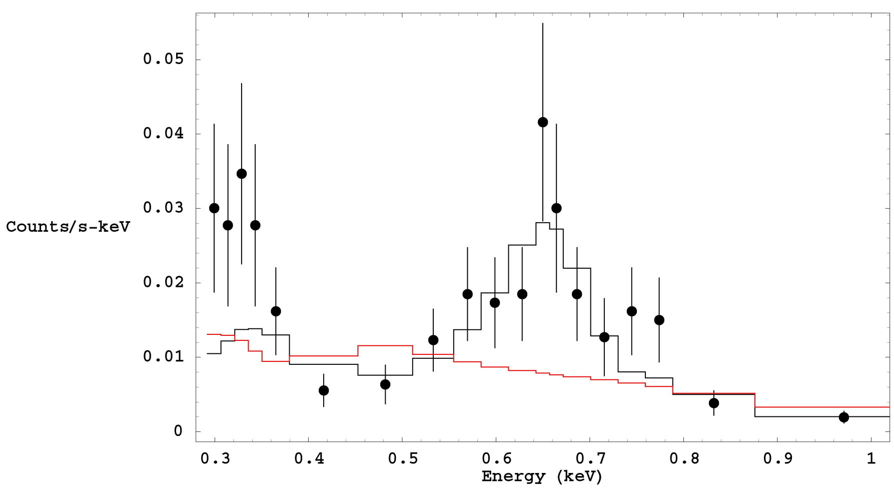

Oxygen & Carbon

Jovian auroral X-ray spectrum between 300 eV and 1 keV of the north auroral region for the first ACIS-S observation. Each spectral point represents ≥ 10 measured events. The red line shows the best-fit bremsstrahlung spectrum, which is clearly inadequate. Jupiter's auroral x-ray emission is due to line emission arising from charge exchange between energetic ions (oxygen with sulfur and/or carbon) and atmospheric neutrals.

The black lines shows best-fit collisional ionization equilibrium models (VAPEC in XSPEC) for O & S (top panel) and O & C (bottom panel), respectively. The O & S model is a better fit, indicating a preference for a magnetospheric origin for the incident ions. XMM-Newton spectra favor O & C, indicating a preference for a solar wind origin.

The spectrum varies in time and can differ from that for the south auroral zone.

45 min Quasi-Periodic Oscillations Observed in Dec, 2000

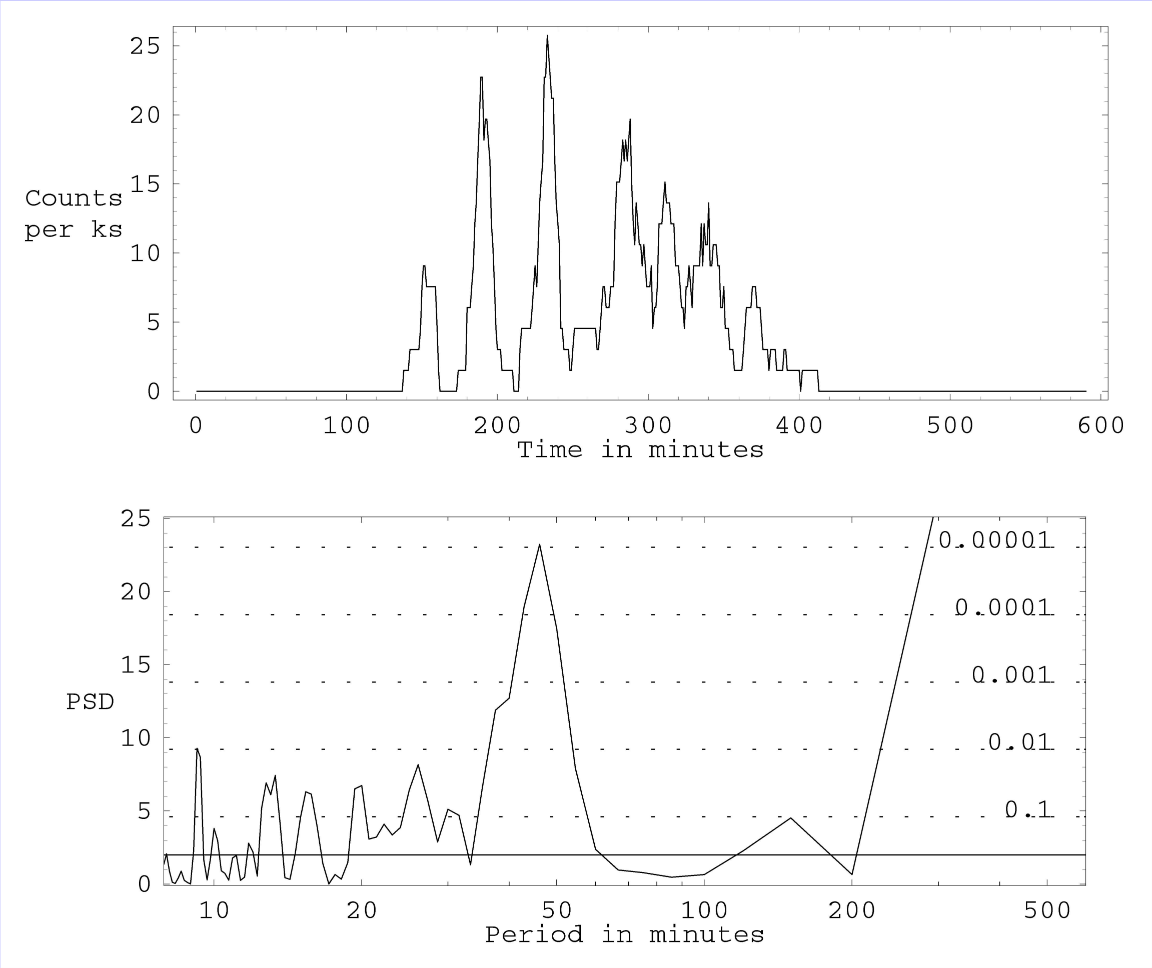

The Dec 18, 2000, HRC-I observations found unambiguous 45 min quasi-periodic oscillations in the x-ray light curve from the northern auroral zone. Quasi-periodic 45 min oscillations in radio emission and in situ energetic particle fluxes have previously been observed by Ulysses and are presumably related.

Auroral Zones Times Series

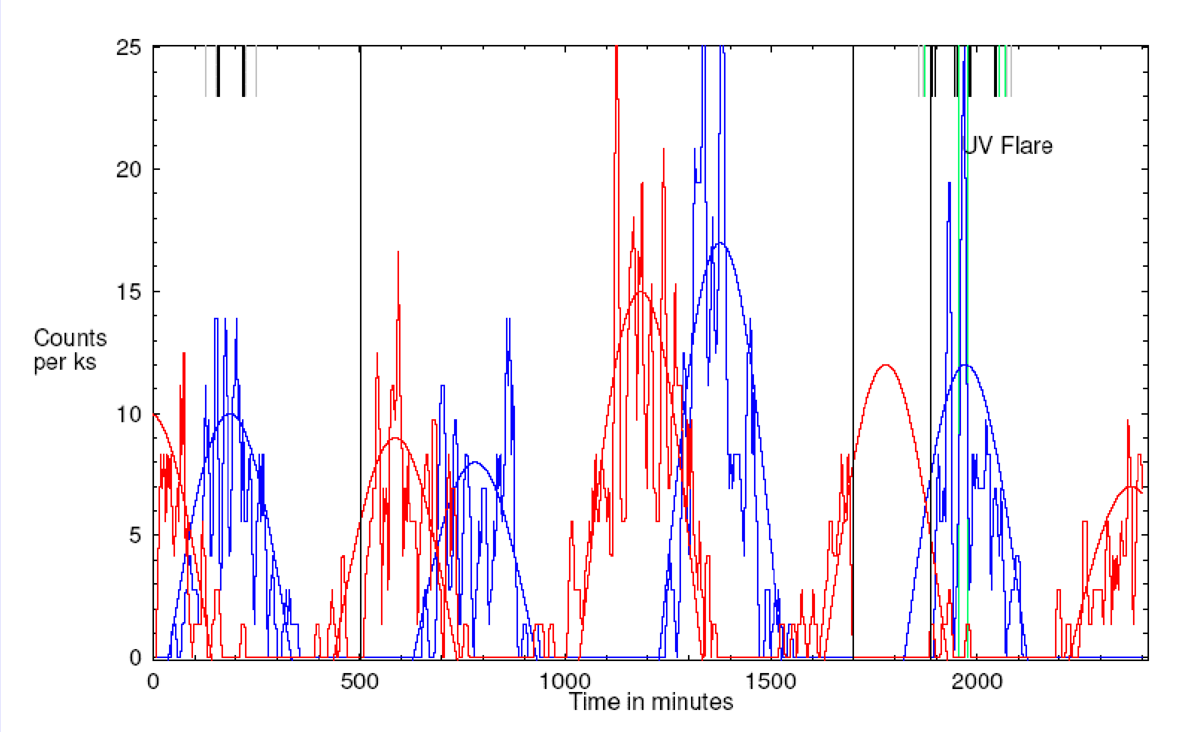

X-ray count rate, in counts per kilosecond, for the northern (blue) and southern (red) auroral zones, created by 12-min boxcar smoothing of a 4-min binning of the data. The time origin corresponds to UT 15:58:06 on 24 February 2003. The black vertical lines from top to bottom mark the transitions from ACIS-S to HRC-I exposures and back to ACIS-S. A gap appears at the beginning of the second ACIS-S exposure because we excised data taken when Jupiter overlapped its location in the second bias frame. The bars at the top mark the simultaneous HST observations. Note that the set of exposures containing the UV flare coincides with the tallest peak in the ACIS-S light curve for the northern auroral zone. Smooth sections of sine waves provide crude representations of projected area effects arising from the planet's rotation.

Timing Analysis for Feb, 2003, Chandra ACIS-S Data

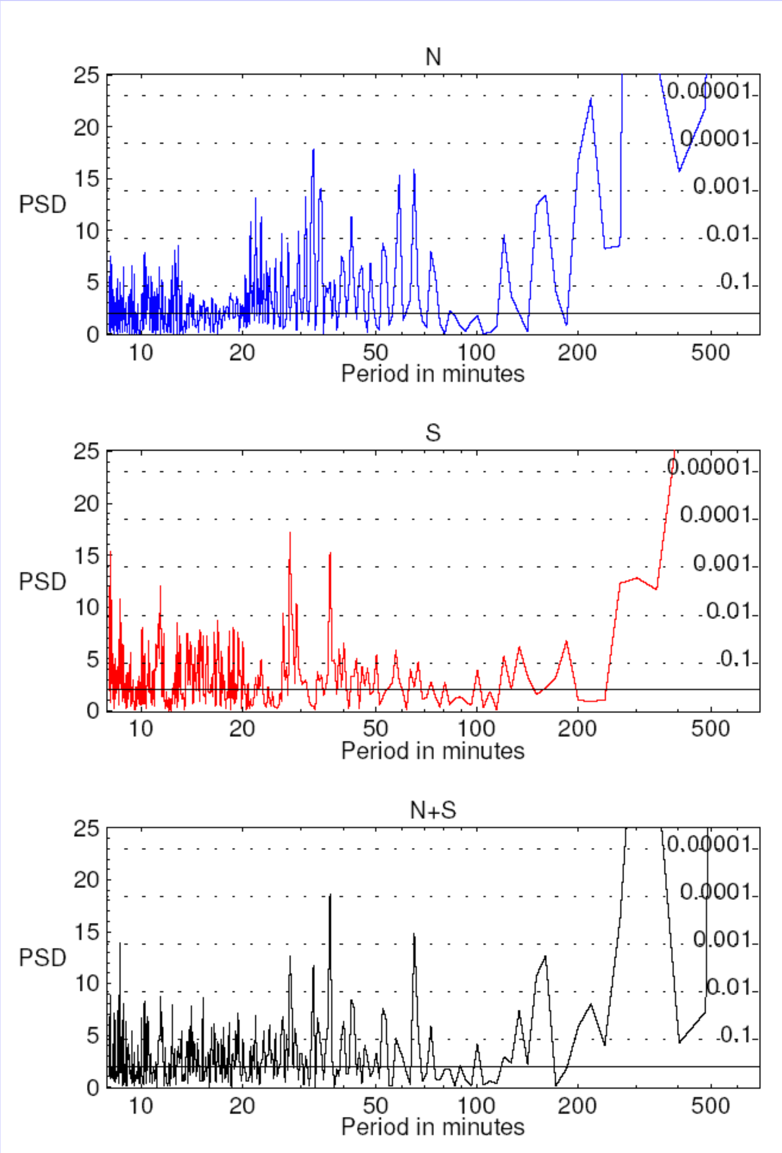

Power spectral density (PSD) versus period (in min), computed from the unsmoothed 4-min binning of the data for the northern (top), southern (middle), and sum of the northern and southern (bottom) auroral zones, respectively. In each plot, the solid line shows the expectation value for a steady source with Poisson statistics. The dotted lines show the single period probabilities of chance occurrence as labeled on the right. There are 217 independent periods between 10 and 100 min (301 in each complete PSD).

Although there is some evidence for chaotic variability, there is no evidence for a strong 45 min quasi-periodic oscillation.

Comparison with Ulysses 10-20 kHz Data

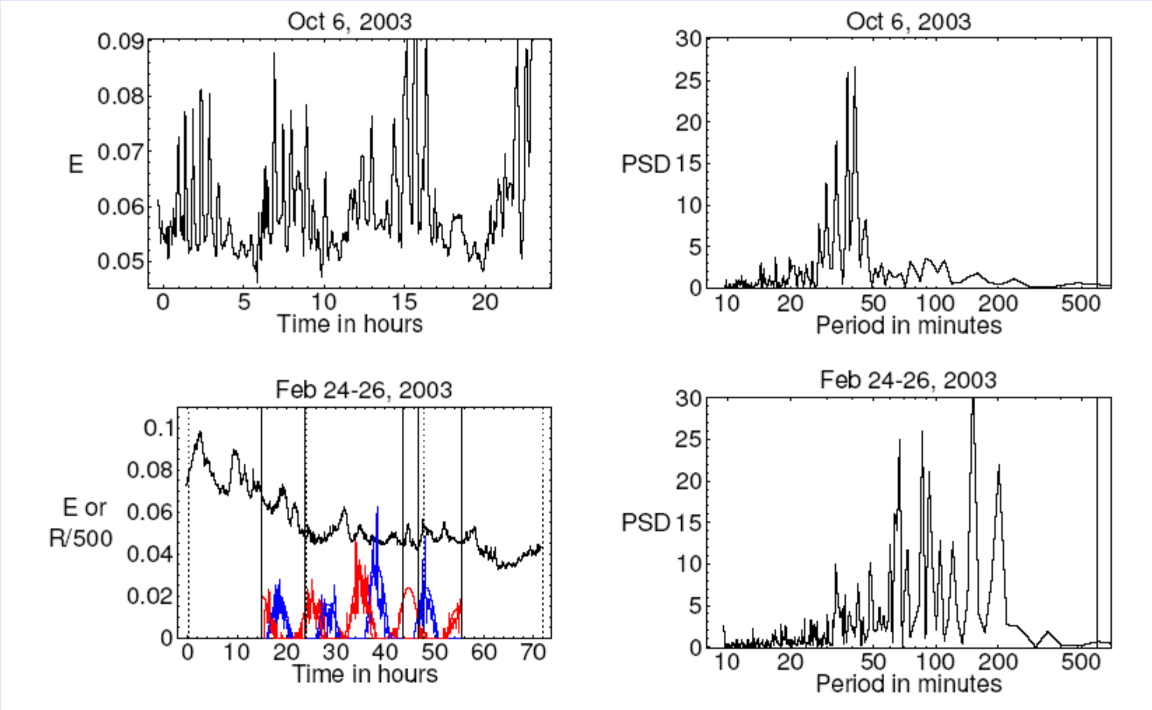

[Right Panel] : PSDs vs. period in min for the Ulysses background subtracted data from **(top)** Oct. 6, 2003, and **(bottom)** 24-26 February 2003. The solid vertical lines mark Jupiter's rotation period. Both PSDs show strong peaks, but that for 6 October 2003, is concentrated in a narrow band near 40 min, while that for 24-26 February 2003, is spread over a wider band above 30 min.

[Left Panel] (Top): Time history for 6 October 2003 of Ulysses integrated electric field, 10-20 kHz, vs. time in hours on 6 October 2003, clearly showing QP40 radio bursts. The data are averaged in 144 s bins. **(Bottom):** In black, the time history of the Ulysses integrated electric field, 10-20 kHz, vs. time in hours on 24 February 2003, 00:00:00, showing the data over a full 3-day interval. The data have been translated back in time from the spacecraft to Jupiter. The solid vertical lines mark the start (1st ACIS-S, HRC-I, 2nd ACIS-S) and the end (2nd ACIS-S) of the Chandra observations. The dotted vertical lines mark the start of each day (24-27 Feb. 2003). Also shown are the Chandra count rates, R/500 where R is in counts per ks, vs. time for the northern (blue) and southern (red) auroral zones. The Chandra data have also been translated back in time from the Earth to Jupiter (the light travel time across the Chandra orbit never exceeds 0.5 s).

Simulataneous FUV and X-ray Auroral Flare

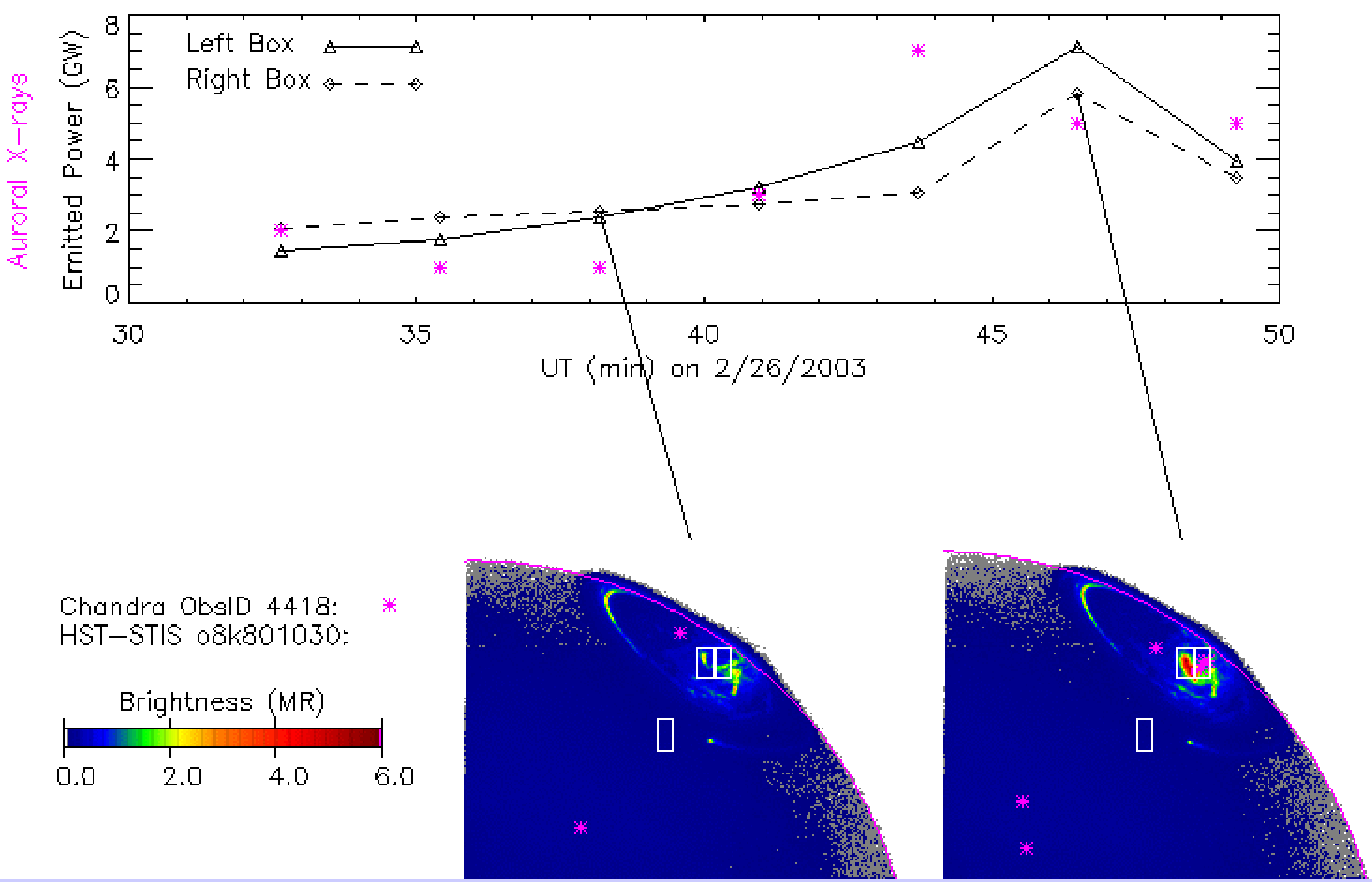

Simulataneous FUV and X-ray Auroral Flare II

The FUV and X-ray light curves (top) and two sample HST-STIS image frames (bottom) for the FUV flare in Jupiter's northern aurora observed on Feb 26, 2003. Each HST-STIS image frame was for 144 s using the FUV MAMA detector with no filter (CLEAR). The frames are separated by 22 s. The FUV flare appears to be mostly confined to the left-hand box while the associated X-rays (shown as pink asterisks) appear mostly in the box on the right. The isolated box was used for disk brightness subtraction. The average number of X-ray counts per 144 s over a two hour span containing the flare is 1.3463; the rise in the number of X-ray counts at the time of the FUV flare is statistically highly significant. The FUV brightness scale is for all emitted FUV H2 and H emissions (not just those in the STIS bandpass), before they are attenuated by the atmosphere (the atmospheric transmission was taken to be 0.4 below 130 nm). The conversion factor for these assumptions is 0.32 counts/s/pixel/MR.

Low- and Mid-Latitude Disk Emission I

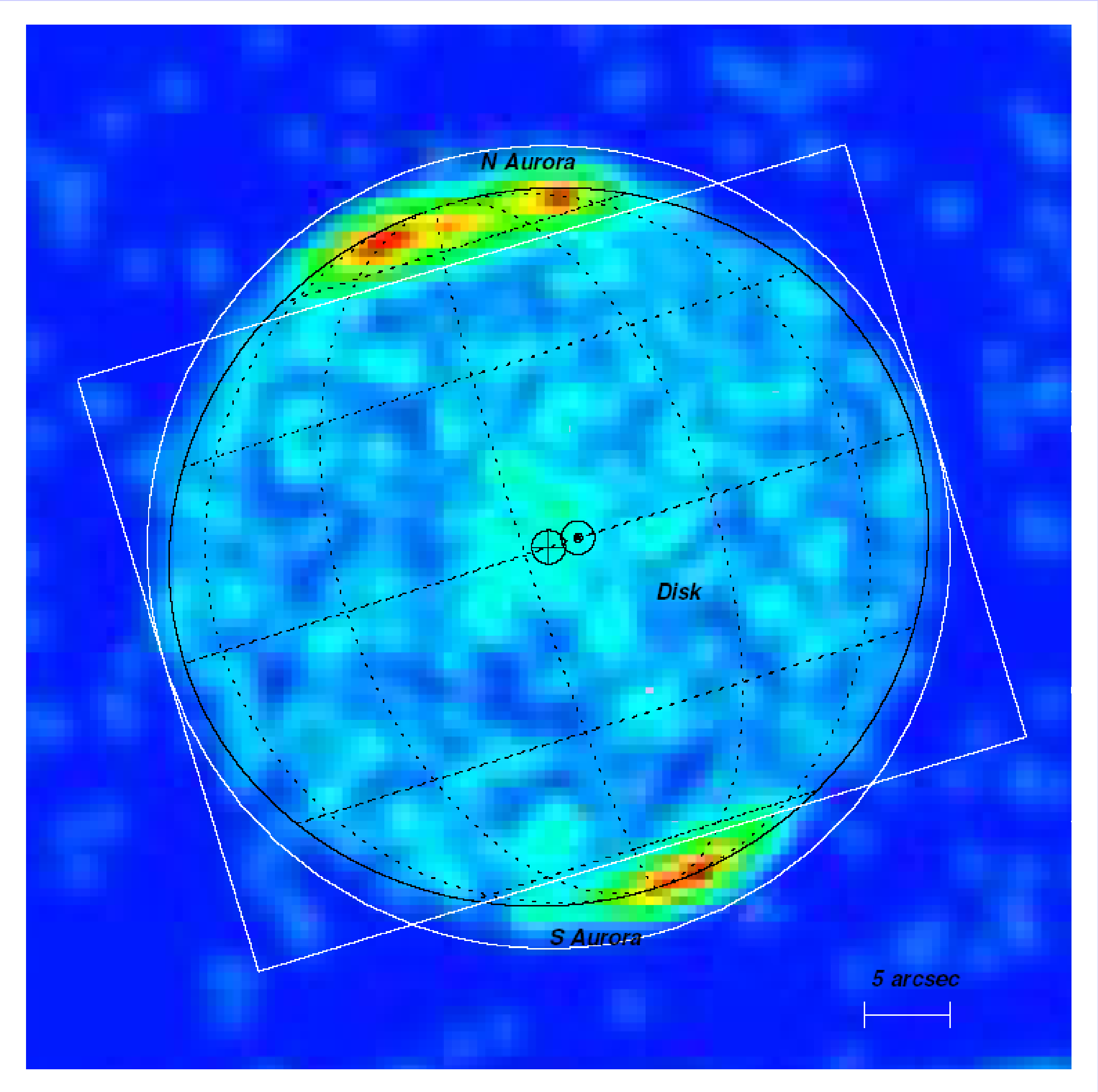

Low- and Mid-Latitude Disk Emission II

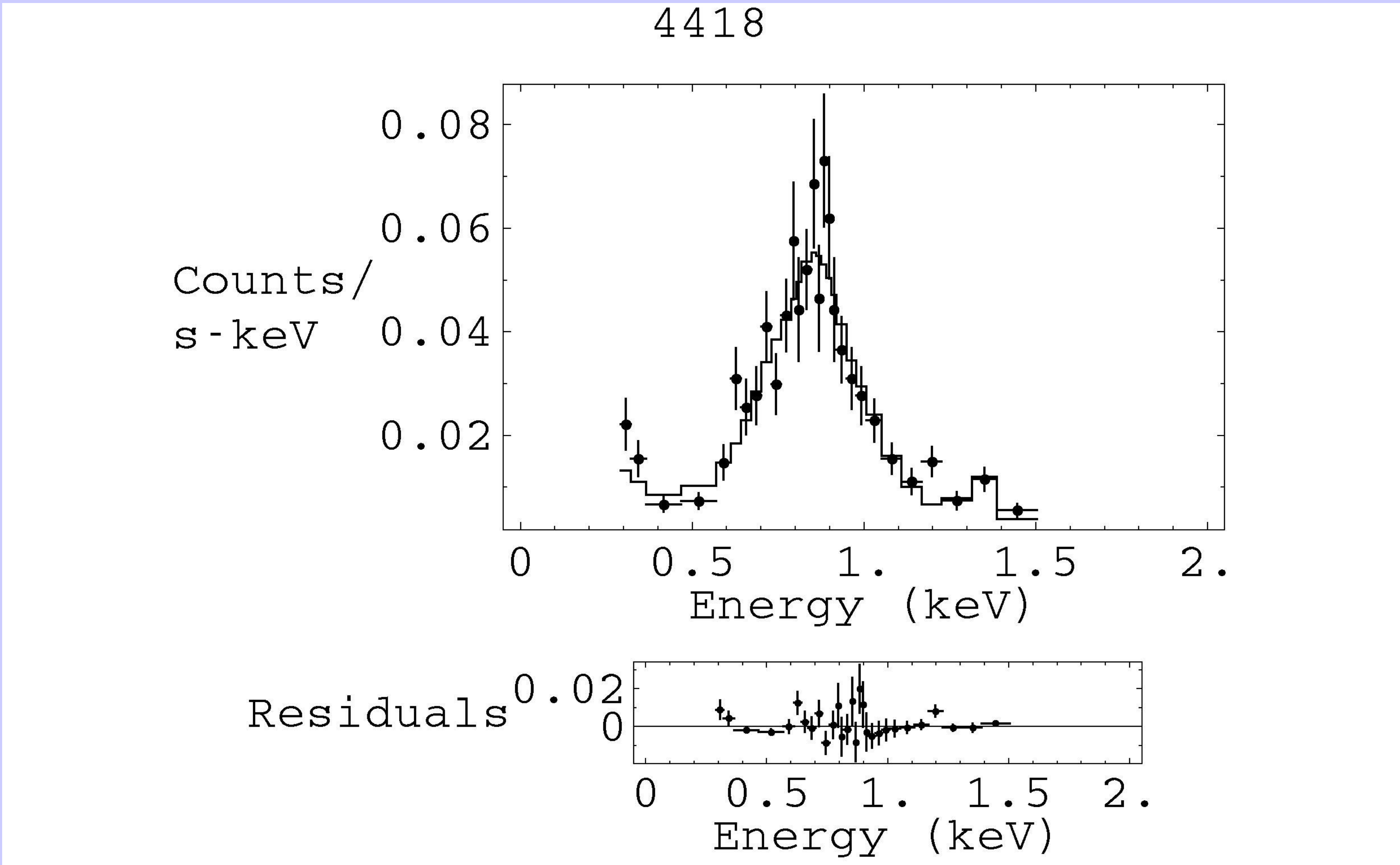

Low- and Mid-Latitude Disk Emission III

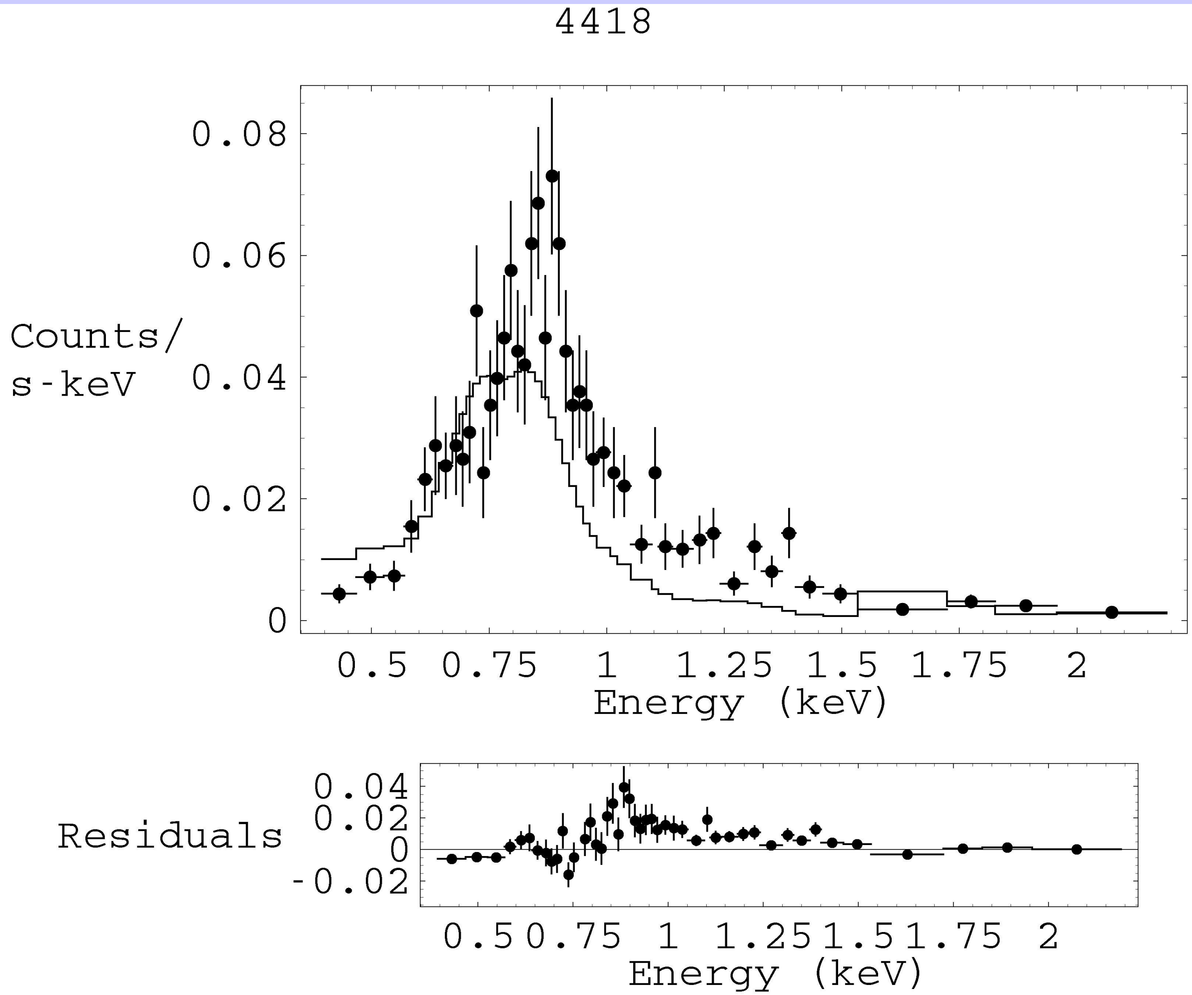

Incident Solar X-ray Spectra

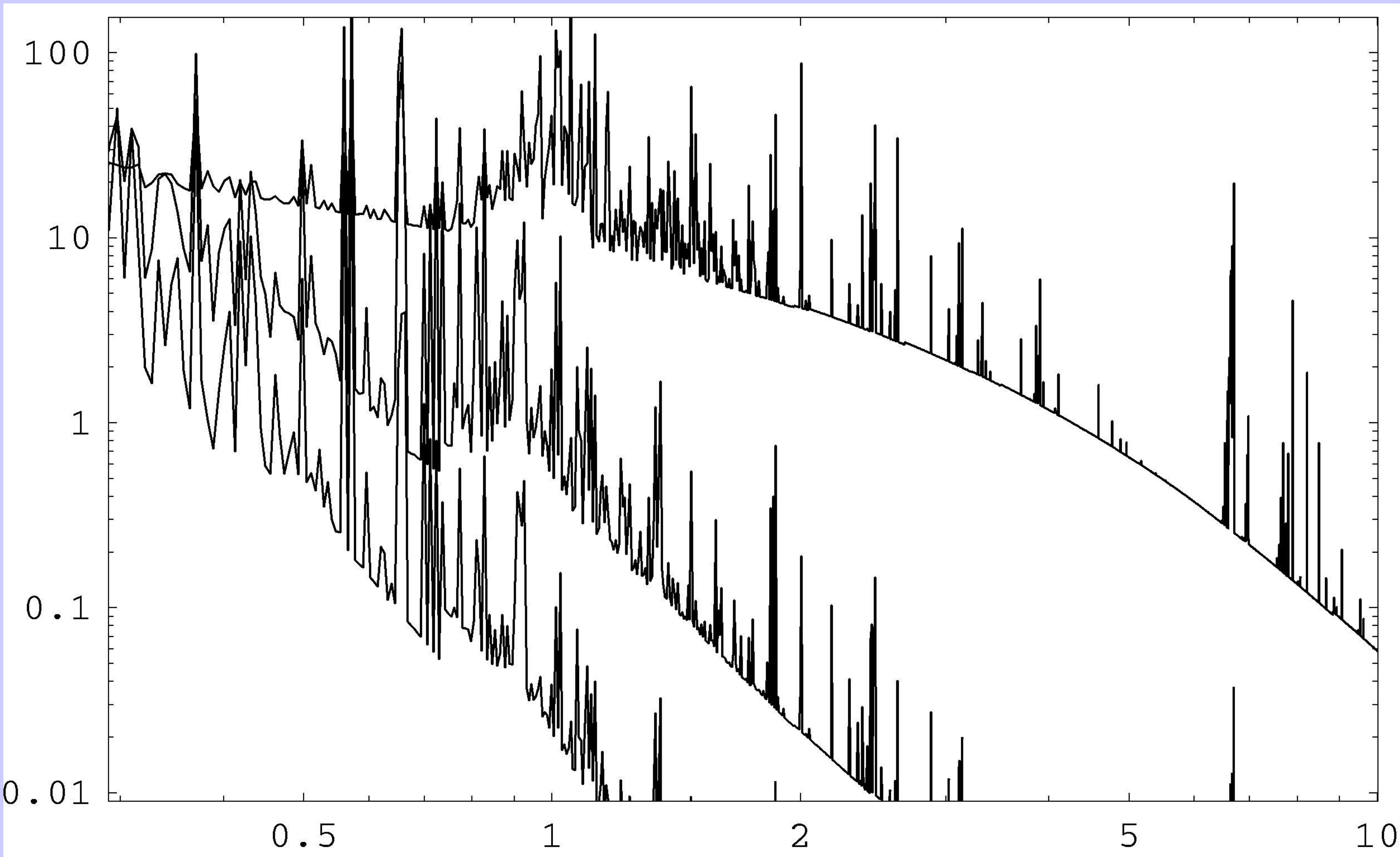

Typical solar x-ray spectra at solar minimum, solar maximum, and during solar flares
(see Peres et al. 2000, Ap. J., 528, 537-551)

How Uniform is the Disk Emission ?

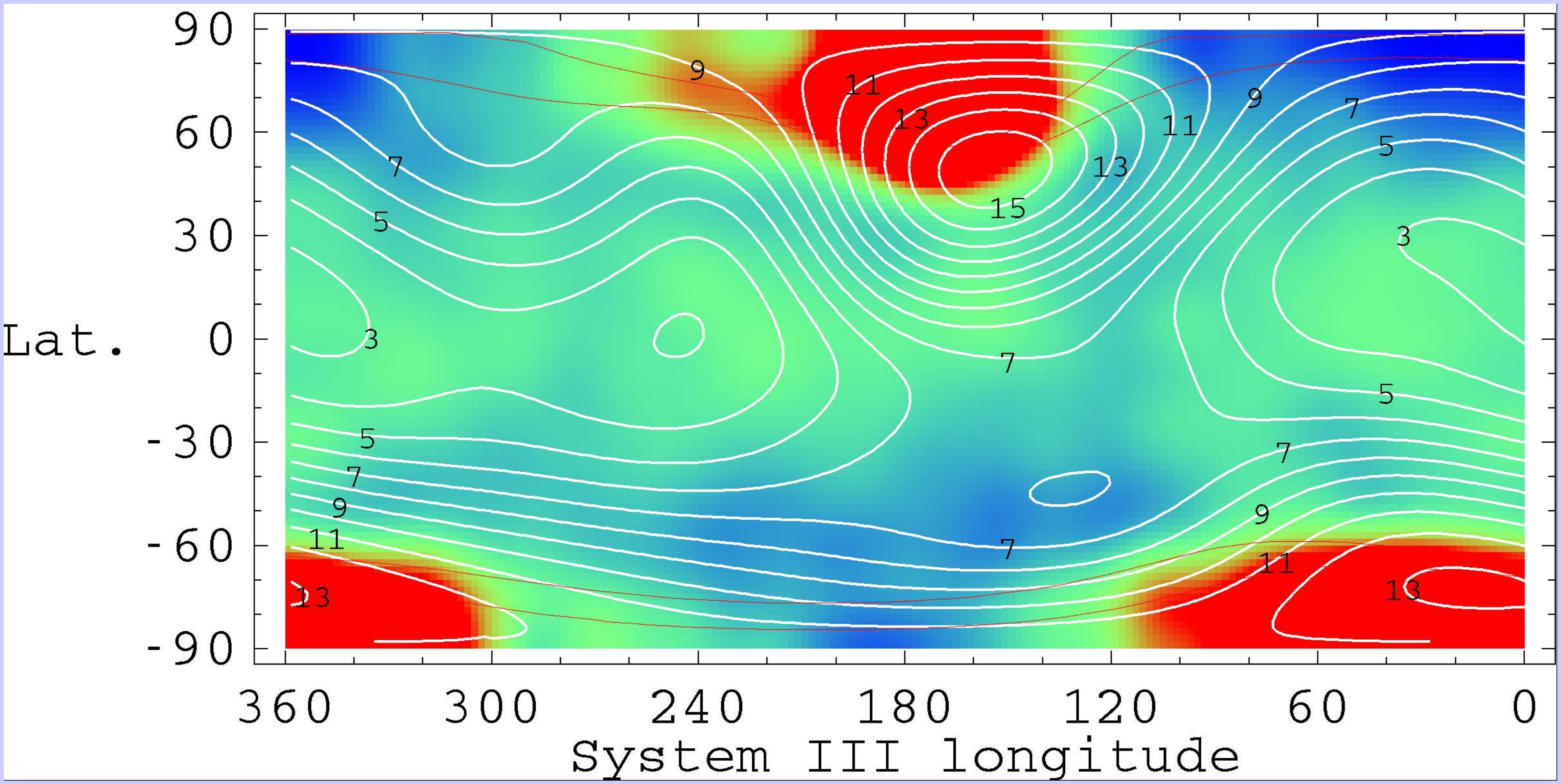

How Uniform is the Disk Emission ?

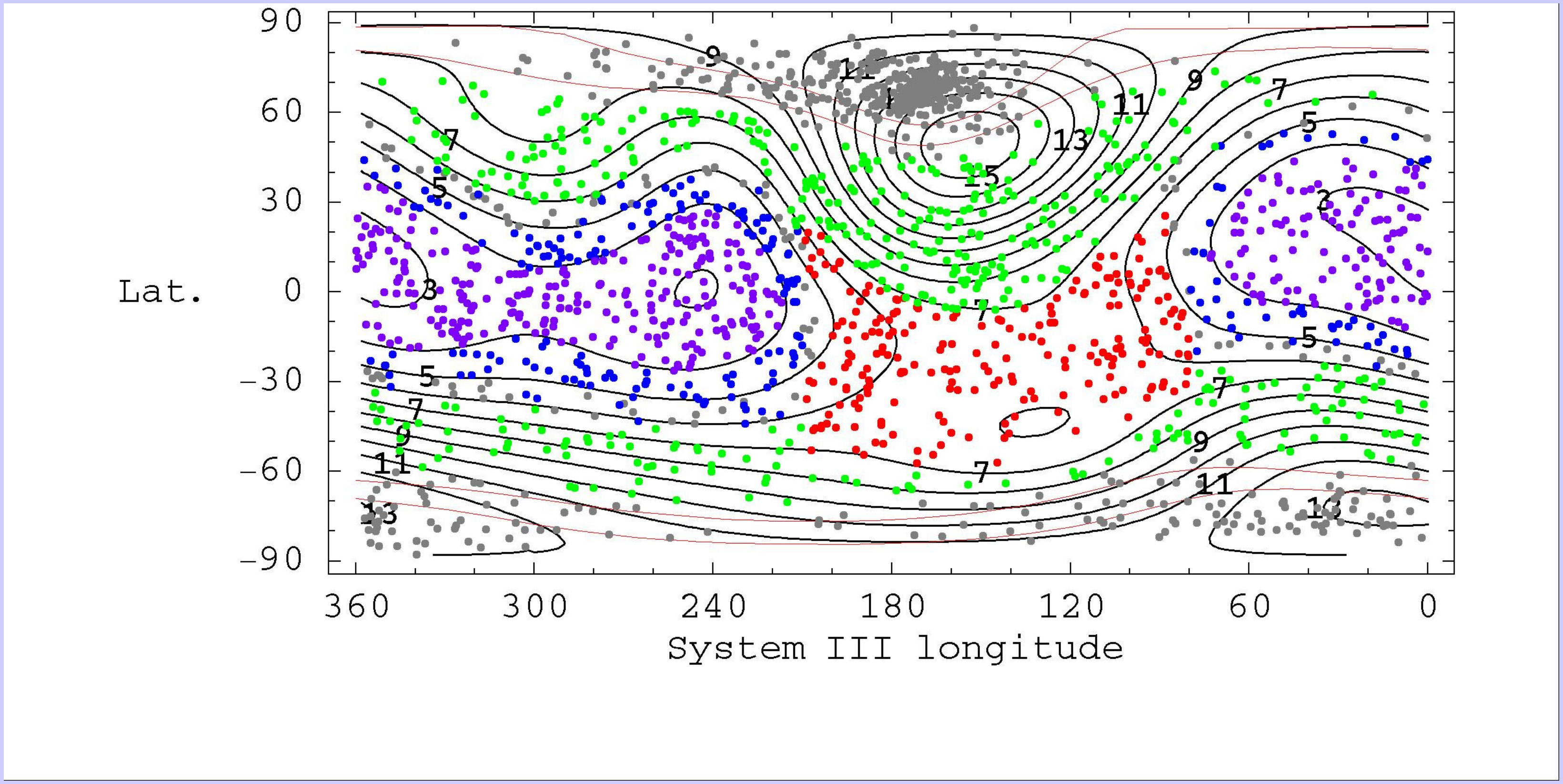

Region 1	Red	5 < B < 7	6.26±0.42	---
Region 2	Purple	B < 4	8.48±0.44	2.22±0.62
Region 3	Blue+Purple	B < 5	9.17±0.38	2.91±0.57
Region 4	Green	Mid-latitudes	6.30±0.31	0.04±0.52

Low-latitude emission may correlate (inversely) with strength of surface magnetic field.
“South-Atlantic anomlies ?

Latitude dependences

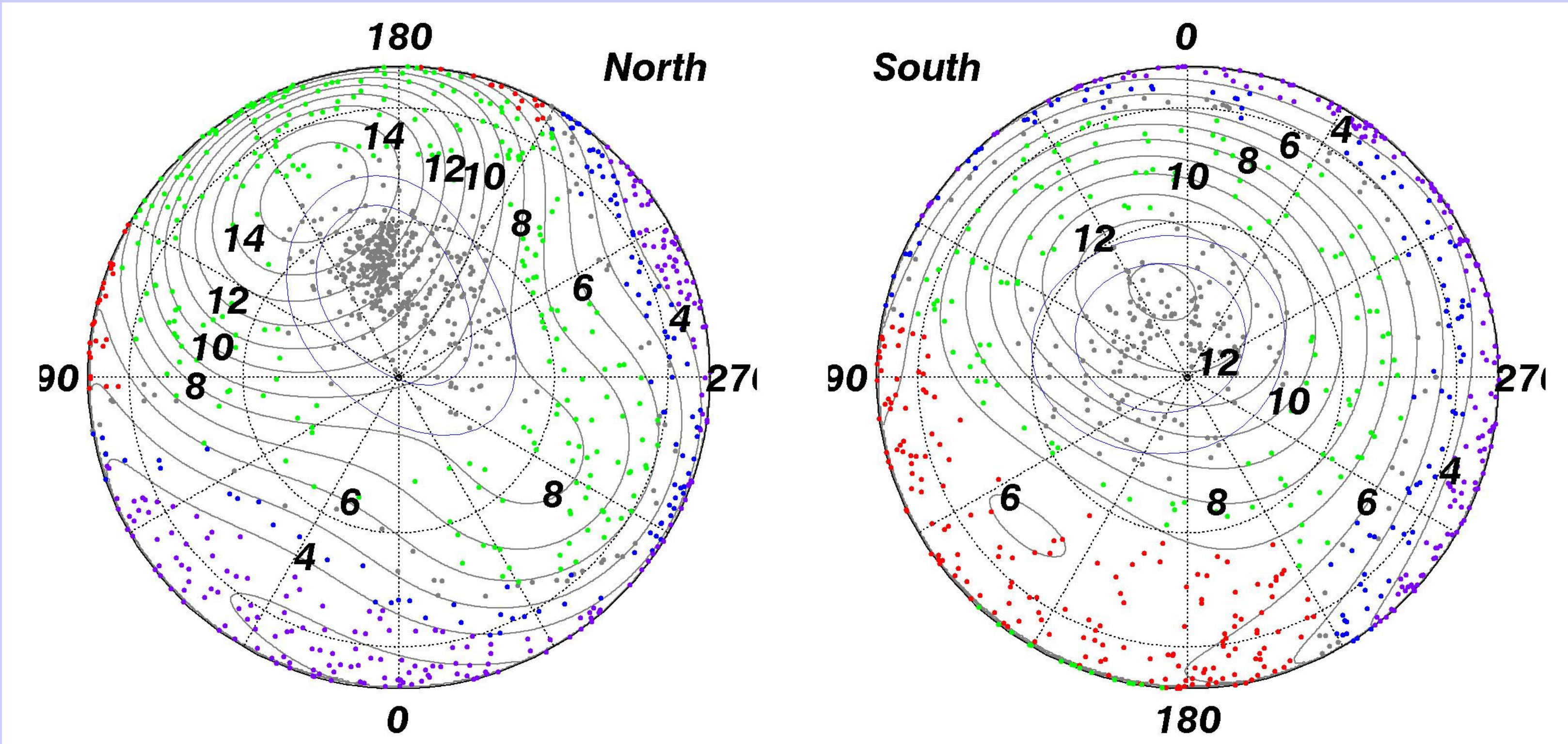

To the extent that the higher field events (red) away from the poles extend to higher latitudes than the low field events (purple, blue), is the result just due to similar dependences on latitude rather than cause and effect?

Spectral Differences

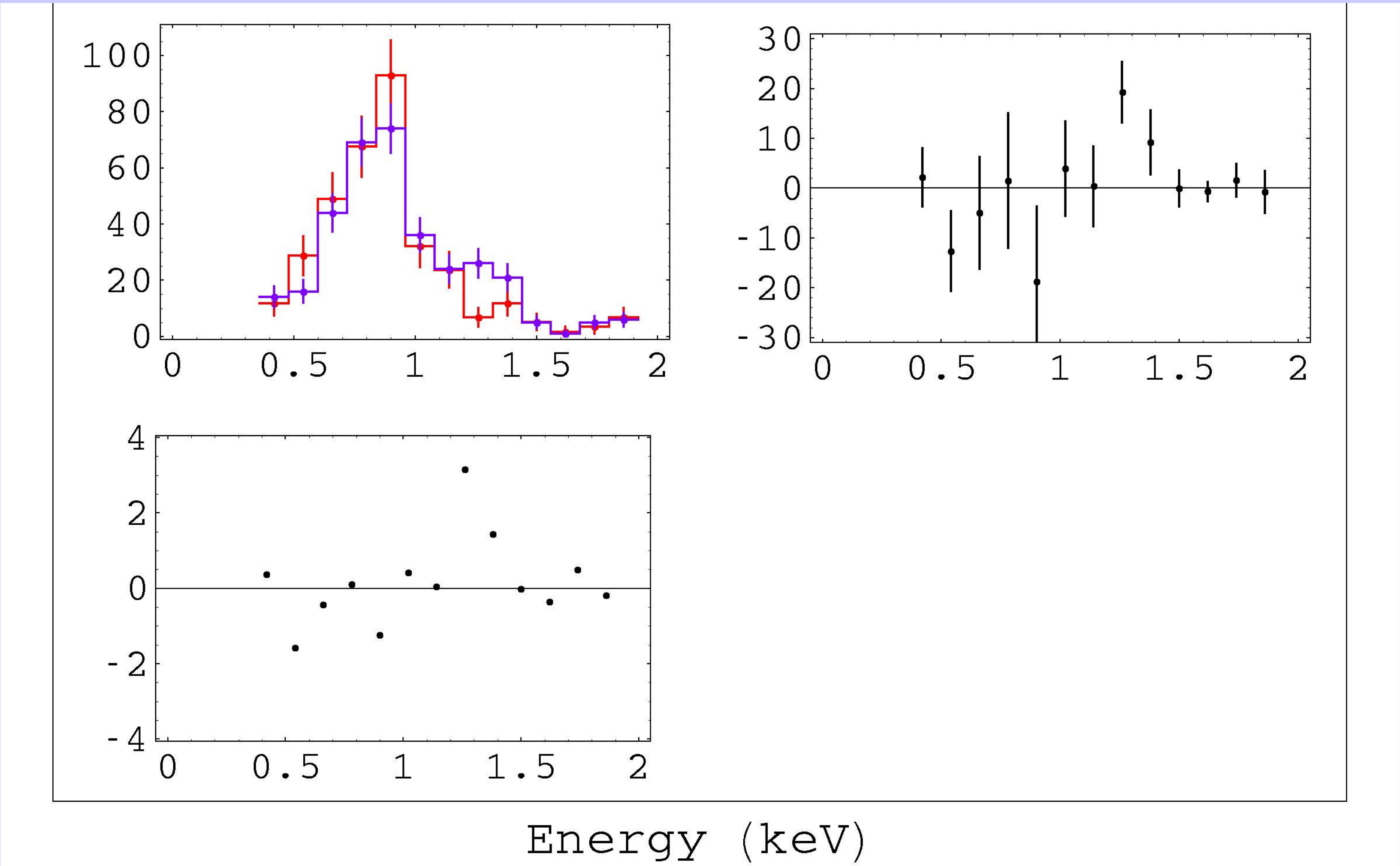

On the other hand, near 1.25 keV there seems to be a real difference in the spectra between regions 1 and 2.

X-ray Emission from the Galilean Moons

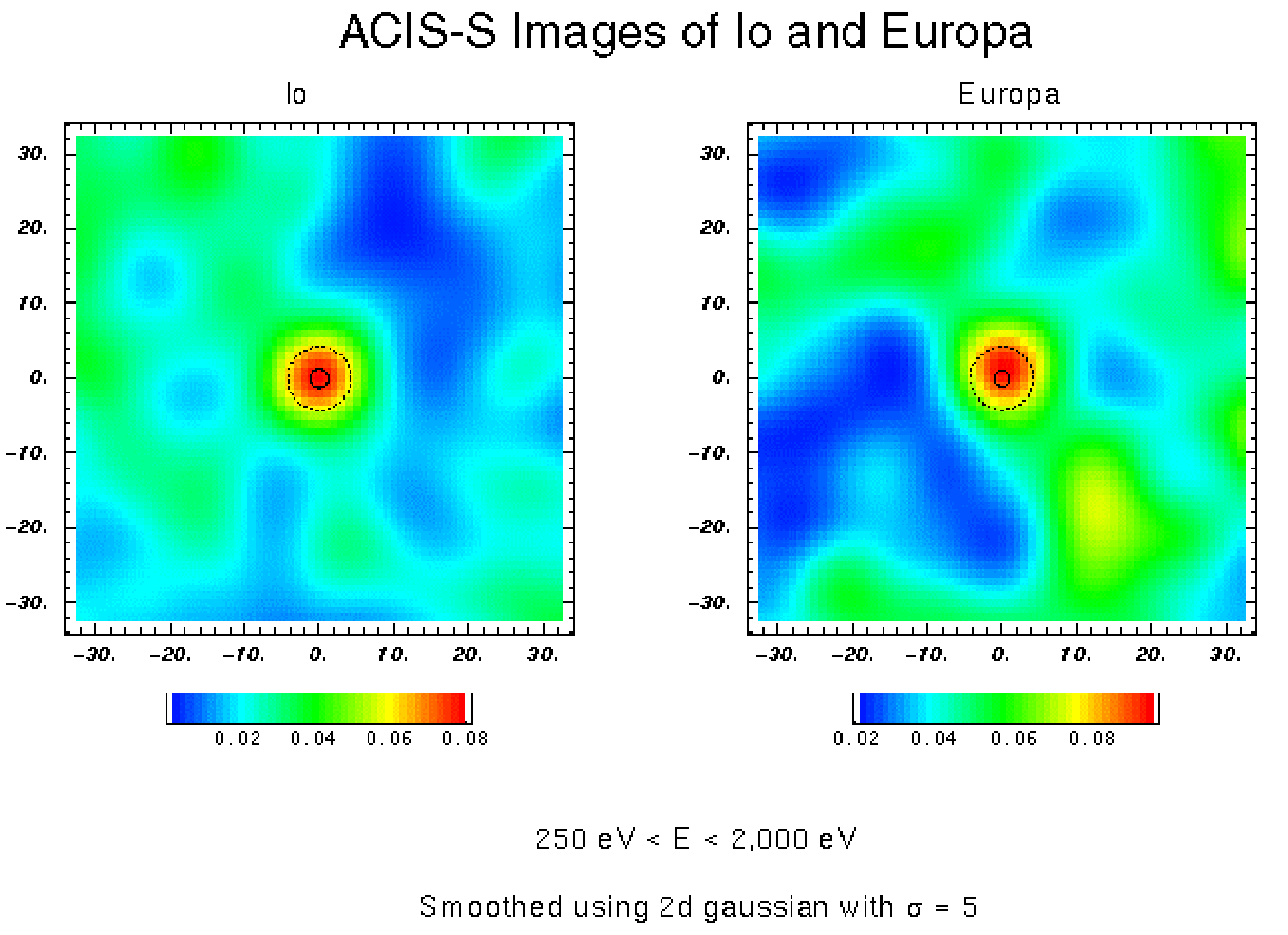

Io and Europa were detected in the 1999 ACIS-S and 2000 HRC-I observations. A large fraction of the events in the ACIS-S data had energies consistent with O-K emission. Ganymede was marginally detected in the 1999 ACIS-S data. These results suggest the possibility of determining the elemental Surface composition of these moons through measuring K shell fluorescence using an in situ instrument.

X-ray Emission from the Io Plasma Torus

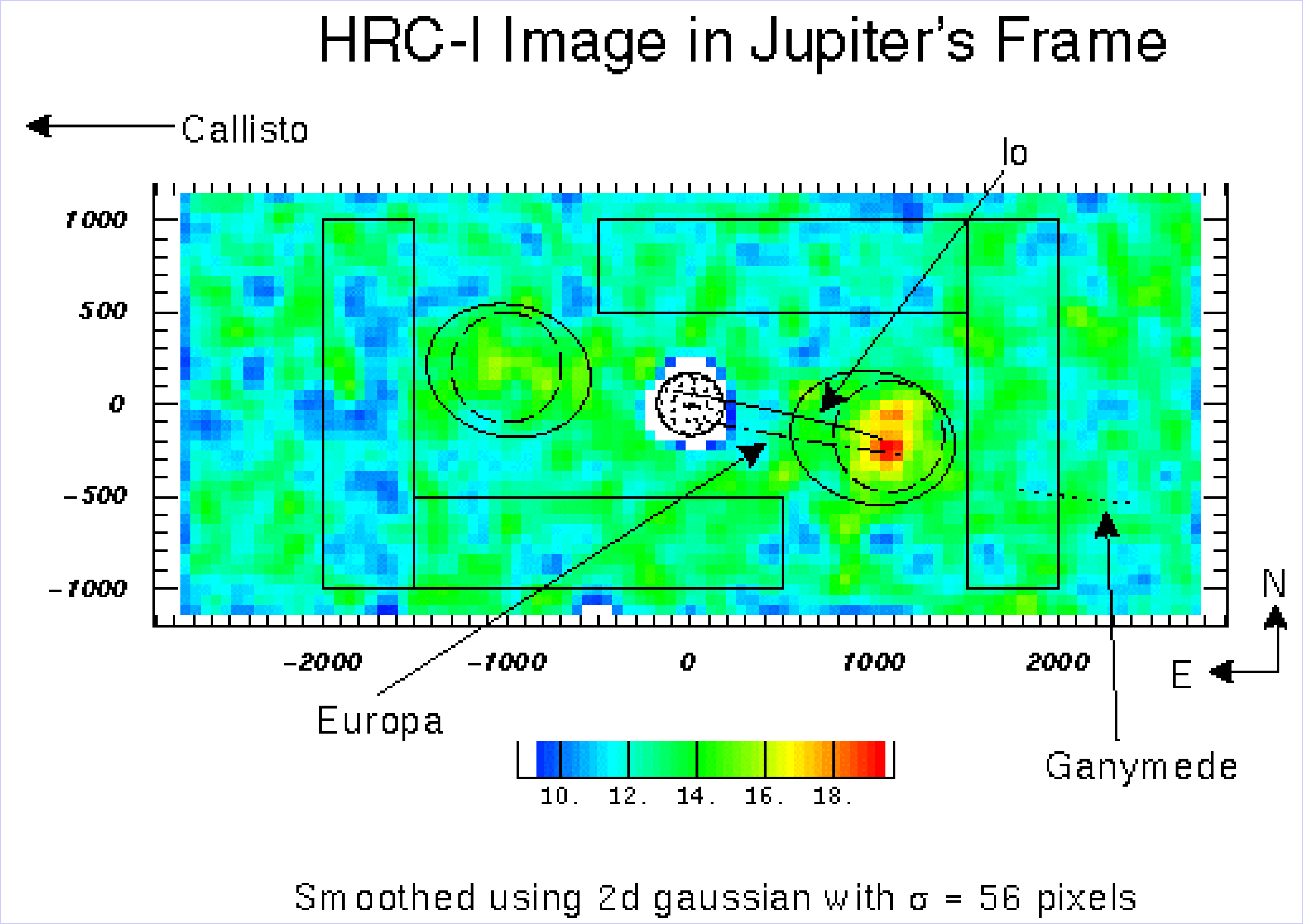

The 1999 ACIS-S and 2000 HRC-I observations also found x-ray emission assoicated with the Io plasma torus. The HRC-I image exhibited the same east-west asymmetry found in the UV. The paths of the Galilean satellites during the observation are also shown.

The X-ray Spectrum of the Io Plasma Torus

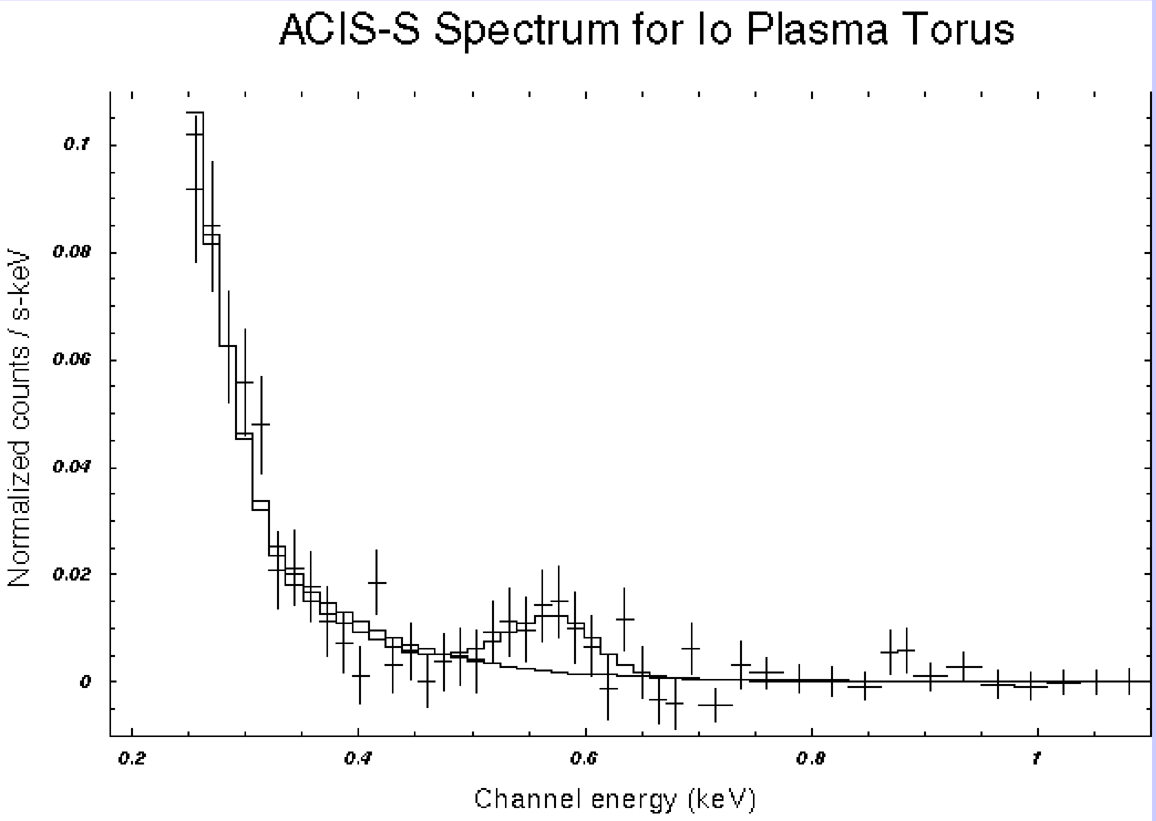

The background subtracted ACIS-S spectrum for the Io plasma torus is well fit by a power law continuum with a steep photon number index of 6.8 plus a gaussian line centered near the energies of O-K lines for several ionization states. The origin of this emission is not well understood, but a large fraction of the continuum flux may result from bremsstrahlung radiation from nonthermal electrons.

The Future

Moon: B. Ramsey (PI), D. Swartz, J. Gaskin, R. Elsner MSFC; G. De Geronimo, P. Rehak, Z. Li BNL; R. Korotev, Wash. U.
Funded

Europa: B. Ramsey (PI), D. Swartz, J. Gaskin, R. Elsner MSFC; J. H. Waite, J. Westlake U. Michigan; J. F. Cooper GSFC; G. De Geronimo, P. Rehak, Z. Li BNL
Submitted Sept 2005

Astrobiology (gasp): J. F. Cooper (PI) GSFC, B. Ramsey, D. Swartz, J. Gaskin, R. Elsner MSFC; J. H. Waite, J. Westlake U. Michigan; and a cast of 1000s
Submitted Oct 2005

Open Questions

1. What is the balance between solar wind entry and magnetospheric plasma precipitation in generating the x-ray aurora and why does the aurora vary?

2. What is the cause of the simultaneous x-ray and UV auroral flares on timescales from 10s of seconds to several minutes?

3. What causes the ~45 minute quasi-periodic oscillations in auroral x-ray emission, radio emission, and relativistic charged particle fluxes? And what mechanism determines whether these phenomena are present or absent?

4. The low-latitude x-ray emission from Jupiter is thought to be largely a response to the incident solar x-ray flux. Are there other contributions? In particular, does the highly non-dipolar nature of Jupiter's magnetic field allow precipitation of energetic particles at low latitudes, forming "anomalies" similar to the South Atlantic anomaly in Earth's magnetosphere?

5. What is the origin of the x-ray emission from the Io plasma torus and why does it vary?

6. Why does the x-ray emission from the Galilean satellites vary?

These questions can be partially addressed, but only partially, by observations of Jupiter over many rotations with the Chandra and XMM-Newton X-ray Observatories.

Opportunities

An imaging x-ray spectrometer operating on a spacecraft approaching and maneuvering in Jupiter's magnetosphere offers a golden opportunity to address these questions in detail, and to study other questions, including details of Jupiter's auroral and low-latitude emission unobtainable from Earth orbit, the x-ray spatial structure and spectra of the faint Io plasma torus, and perhaps most importantly the elemental surface composition of the icy Galilean satellites and Io as well.

The x-ray emission from Jupiter and the Io plasma torus could be studied from a safe distance outside Jupiter's fierce radiation belts. For example, a region with radius 2 times Jupiter's fits inside a 2 degree field of view at a distance of 115 Jupiter radii from the planet, a factor 90 times closer than Jupiter and Earth at opposition. A region with radius 20 times Jupiter's (thus including the Io plasma torus) fits inside a 2 degree field of view at a distance of 0.5 AU, a factor 9 times closer than Jupiter and Earth at opposition.

Spatially and temporally resolved measurements of the flux and spectra from Jupiter's aurora seem possible, as do searches for x-ray emission from the feet of satellite flux tubes. These types of measurements are impossible to do from Earth orbit for the foreseeable future.

JPL Study of a Europa Geophysical Orbiter

http://www.lpi.usra.edu/opag/jun_05_meeting/presentations/EGE_Science_Instruments_Trace_OPAG.pdf

Mission Objective	Techniques	Instruments	Remarks
A. Confirm the presence of a sub-surface ocean	Geodesy, induced fields, surface motion, libration, surface deformation	Precision tracking, altimeter, imager, magnetometer, SAR [Seismometer] [Supporting measurements for magnetometer	SAR – insufficient power to operate with other radars Altimeter – Topomapper desirable, imager needed Seismometer – requires lander
B. Characterize the three-dimensional configuration of the icy crust, including possible zones of liquid	Multi-frequency sounding, altimetry, mapping, gravimetry	Sounder, mapping altimeter, imager, SAR, precision tracking (at low altitude)	Single frequency sounder and sub-sampled altimetry in baseline
C. Map the organic and inorganic surface compositions, especially as related to astrobiology	UV, VIS, IR spectroscopy, Neutral and ion spectroscopy **X-ray spectroscopy**	IR, mapping spectrometers, neutral and ion spectrometers for several energy ranges, **X-ray spectrometer**	**X-ray requires development, possible detector challenges** Neutral and ion spectroscopy and mapping spectroscopy reduced in baseline
D. Characterize surface features and identify candidate sites for future exploration	Multi-band image mapping, topography, thermography, photometry	Multi-band VIS mapper, altimeter, radiometer	Radiometer and topomapper not in baseline Difficult to accommodate photometry
E. Characterize the magnetic field and radiation environment	Magnetic fields, electrons, ions and neutrals	Magnetometer, ion and neutral spectrometers for low and high energy, UV and IR photometers	High energy resolution low in baseline Difficult to point into co-rotating plasma
F. Understand the heat source(s) and time history of Europa's ocean	Gravity fields, mapping, altimetry, fields and particles, spectroscopy	Correlate measurements from objectives A, C, and E Dust	Dust not in any payload configuration

Mapping the Elemental Surface Composition of the Icy Moons

Jupiter’s icy moons, Europa, Ganymede, and Callisto, are located within its radiation belts. Energetic particles in these belts bombard each moon’s surface, producing fluorescent x-ray emission from the surface materials, in addition to bremsstrahlung.

In principle, high-resolution spatial and spectral x-ray measurements from an orbiting spacecraft could determine the elemental composition of these surfaces in detail.

Mapping the elemental surface composition of the icy Galilean satellites is challenging.

Principal Challenge I: Radiation Environment

The very harsh radiation environment means:

1. Large accumulated dose (~0.25 Mrad over 2-3 months) expected even with substantial shielding.

2. Very high count rates (mostly background) require high speed operation.

Focusing optics are required to reduce detector size, and x-ray CCDs are ruled out.

There is possibility of life on Europa or in its subsurface oceans, so measurement of C K-shell line is highly desirable, requiring low threshold (0.2 keV) and high energy resolution (<150 eV FWHM).

The solution may be arrays of silicon PIN diodes or drift detectors with custom readout electronics, such as those developed at BNL, as the focal plane detectors.

1. Single silicon wafer contains hundreds of individual detector elements (pixels).

2. Each detector has its own electronics readout channel, implying high rate capability. Low capacitance means good energy resolution. No clocking of charge packets so very radiation resistant.

Principal Challenge 2: Background & Sensitivity

1. Adopting incident electron, proton, and heavy ion fluxes consistent with in situ Galileo measurements, one of us (DAS) carried out GEANT simulations to determine the expected background when orbiting Europa. If the telescope aperture is left open, the background is completely dominated by contributions due to electrons entering the aperture. A magnetic broom such as used on Chandra would not have a sufficient "lever arm" to provide sufficient shielding.

Possible solution: An entrance window thin enough to permit measurements at C Kα (~280 eV).

2. Assuming a 1.2 m telescope, with 49 mirror shells, ~390 cm^2 geometric area, and a 2^o FWHM field of view, even if the background is kept down to $2\ 10^3$ cts/s-cm^2, measurement of abundances relative to oxygen below 1% (<0.2% for F through Cl) requires ~7.5 ks for a region 3 km diameter on Europa's surface, assuming a spacecraft altitude of 100 km.

This means complete coverage of Europa's surface is not possible within a mission lifetime of 30 days. The ~1.4 km/s relative velocity between the spacecraft and the ground (at 100 km altitude) further implies that only the equatorial regions (for low inclination orbits) or polar regions (for high inclination orbits) could be mapped at the highest sensitivity and spatial resolution. However …

Europa surface coverage from 100 km I

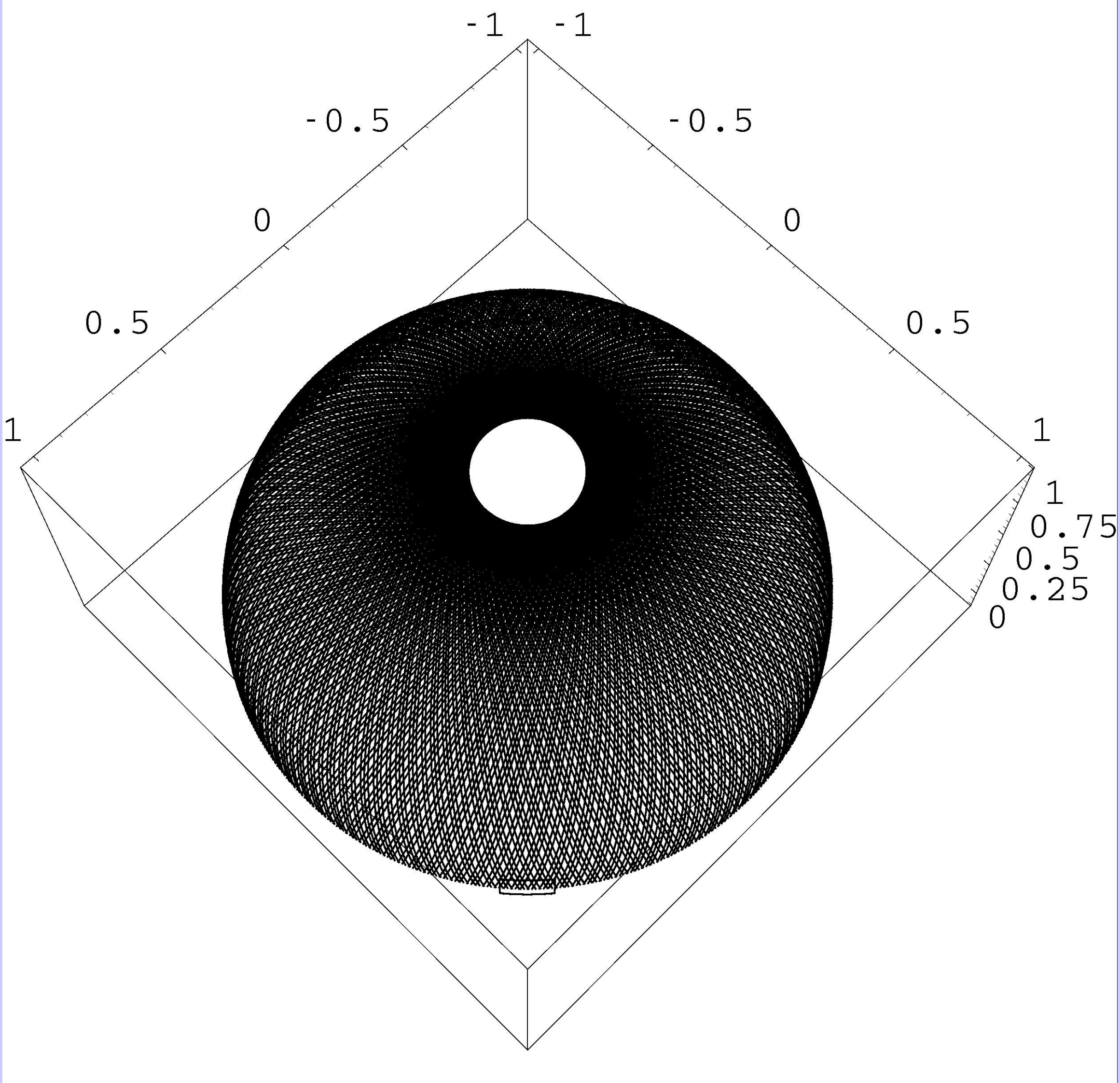

Europa surface coverage from 100 km II

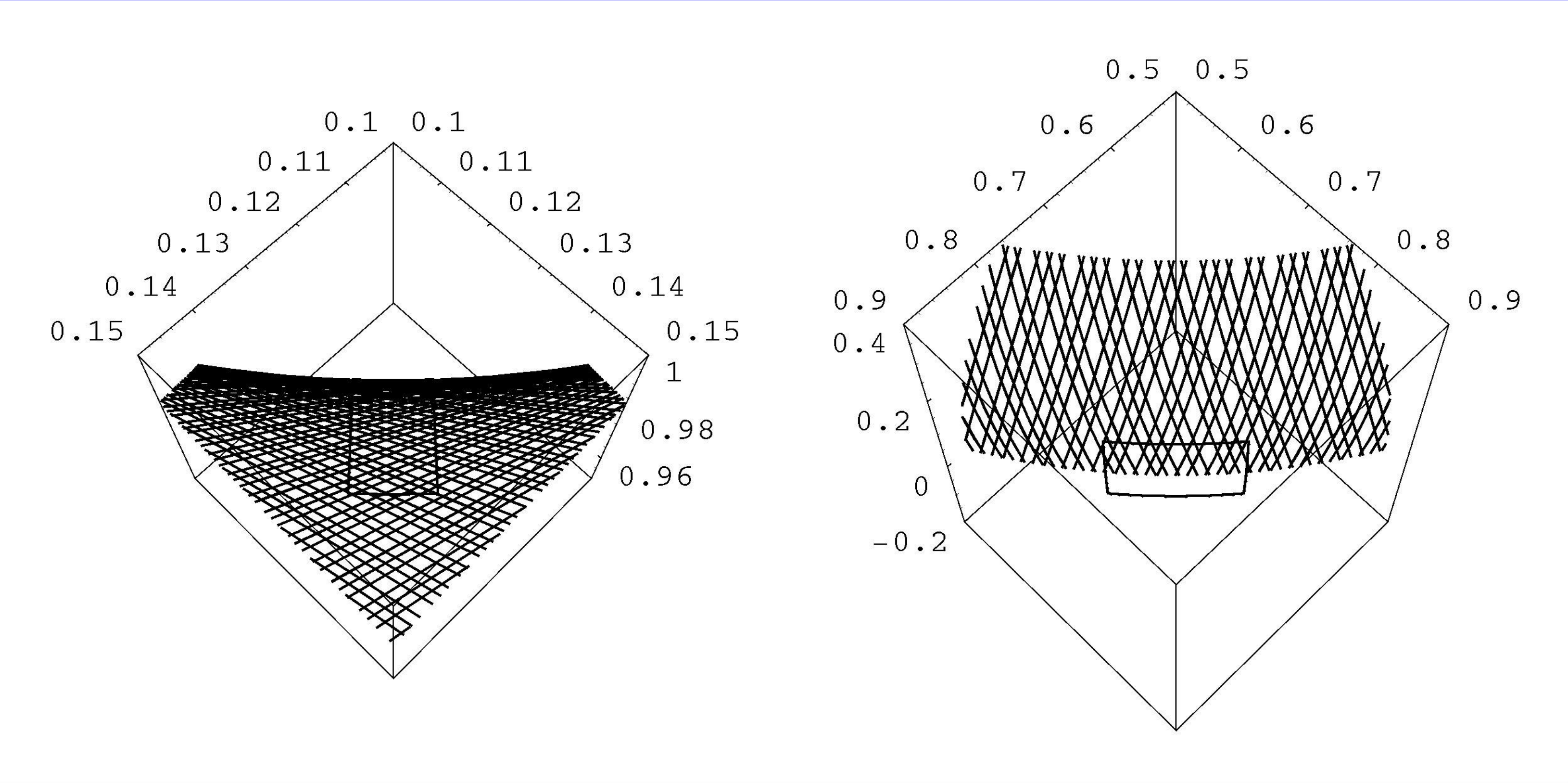

Expected Sensitivies for Elements on the Surfaces of Europa and Io

Sensitivity can be built up in a sector by adding together data from orbits crossing it. If we assume a flux in O Kα equivalent to that observed by Chandra, line fluxes proportional to fluorescent yield, and an integration time per sector of 7.5 ks, then for 1 month in an 80 degree inclination orbit at 100 km, the instrument configuration we described can reach the 3σ limiting abundances relative to O given on the right for Europa in sectors that are 96×141 km at high latitude and 540×540 km at the equator, giving a total of ~200 image elements covering the surface between ±80 degree latitude. For mission lifetimes extending beyond 1 month, our sensitivities improves as $t^{-1/2}$.

If the spacecraft has the ability to point at Io from Europa orbit, then the 3σ limit abundances listed for Io, integrated over the moon's surface, are achievable in an exposure time of 1.77 d (Io's orbital and rotational period).

Element	**Energy (keV)**	**Effective Area (cm^2)**	**% abundance relative to oxygen**	
			Europa	**Io**
Carbon	0.277	276	0.65	0.40
Nitrogen	0.392	275	0.35	0.22
Fluorine	0.677	263	0.15	0.09
Neon	0.849	189	0.16	0.09
Sodium	1.040	168	0.15	0.08
Magnesium	1.254	178	0.11	0.06
Aluminum	1.487	174	0.08	0.04
Silicon	1.740	156	0.08	0.04
Potassium	2.014	105	0.12	0.05
Sulfur	2.308	70	0.18	0.06
Chlorine	2.622	62	0.18	0.05
Calcium	3.692	38	0.26	0.05
Iron	6.404	6.5	1.05	0.12

An Alternate Solution

One of us (JFC) has suggested that locating an imaging x-ray spectrometer in orbit around Ganymede might be an ideal location for long-term studies of the Jovian system:

1. The radiation environment is more benign, with fluxes an order of magnitude less than at Europa.

2. Ganymede is of intrinsic interest as the largest moon in the solar system and possesses its own mini-magnetosphere.

An angular resolution of 1.5 arcmin and an altitude of 100 km implies a surface resolution for Ganymede of ~40 m. If necessary, sensitivity could be increased by combining resolution elements.

For remote sensing of Europa and Io from Ganymede at minimum separation distances of 5 and 9 Jupiter radii, respectively, the surface resolution would be 140 and 260 km, respectively. As the radii of Europa and Io are 1565 and 1820 km, respectively, compositional mapping of distinct geological regions would be possible.

Goodnight Mrs. Kalabash, wherever you are.

- Jimmy Durante